ORIGINAL RESEARCH

Senescence Connects Autophagy Deficiency to Inflammation and Tumor Progression in the Liver

Nazmul Huda,[1] Bilon Khambu,[1,2] Gang Liu,[1,2] Hirokazu Nakatsumi,[3] Shengmin Yan,[1,2] Xiaoyun Chen,[1] Michelle Ma,[2] Zheng Dong,[4,5] Keiichi I. Nakayama,[3] and Xiao-Ming Yin[1,2]

[1]Department of Pathology and Laboratory Medicine, Indiana University School of Medicine, Indianapolis, Indiana;
[2]Department of Pathology and Laboratory Medicine, Tulane University School of Medicine, New Orleans, Louisiana;
[3]Department of Molecular and Cellular Biology, Medical Institute of Bioregulation, Kyushu University, Fukuoka, Japan;
[4]Department of Cellular Biology and Anatomy, Medical College of Georgia at Augusta University, Augusta, Georgia; and
[5]Research Department, Charlie Norwood VA Medical Center, Augusta, Georgia
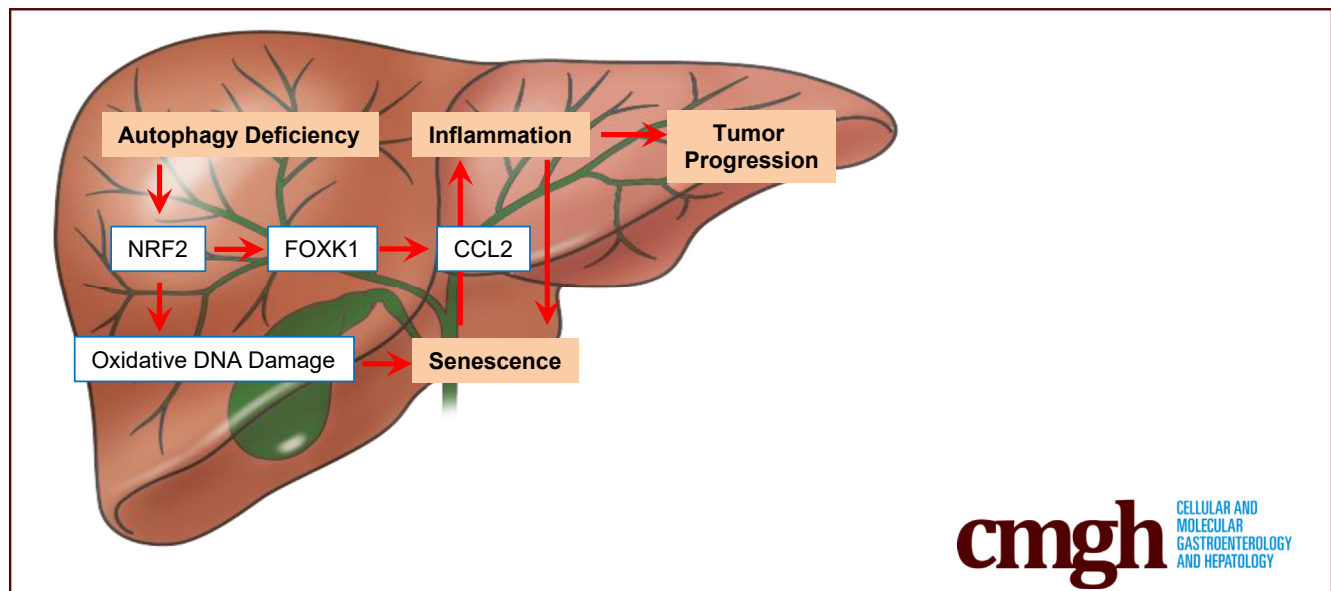
SUMMARY

Senescence is rapidly induced in autophagy-deficient livers in a nuclear factor erythroid 2-related factor 2–dependent way and induces inflammation through the nuclear factor erythroid 2-related factor 2– forkhead box K1–C-C motif chemokine ligand 2–C-C motif chemokine receptor 2 pathway, which in turn further enhances senescence and inflammation, and affects liver injury and tumor development.

BACKGROUND & AIMS: Cellular senescence frequently is present in injured livers. The induction mechanism and the pathologic role are not always clear. We aimed to understand the dynamics of senescence induction and progression, and the mechanism responsible for the pathology using a mouse model that disables the essential process of autophagy.

METHODS: Mice deficient in key autophagy genes *Atg7* or *Atg5* in the liver were used. Senescence was measured using established cellular and molecular signatures. The mechanistic roles of nuclear factor erythroid 2 (NRF2), forkhead box K1, and C-C motif chemokine receptor 2 (CCR2) were assessed using mouse genetic models. Liver functions, pathology, and tumor development were measured using biochemical and histologic approaches.

RESULTS: Inducible deletion of *Atg7* rapidly up-regulated cyclin-dependent kinase inhibitors independently of injury and induced senescence-associated β-galactosidase activities and senescence-associated secretory phenotype (SASP). Sustained activation of NRF2 was the major factor causing senescence by mediating oxidative DNA damage and up-regulating C-C motif chemokine ligand 2, a key component of autophagy-related SASP, via the NRF2–forkhead box K1 axis. Senescence was responsible for hepatic inflammation through CCR2-mediated recruitment of CD11b$^+$ monocytes and CD3$^+$ T cells. The CCR2-mediated process in turn enhanced senescence and SASP by up-regulating cyclin-dependent kinase inhibitors and chemokines. Thus, senescence and inflammation can mutually augment each other, forming an amplification loop for both events. The CCR2-mediated process also modulated liver injury and tumor progression at the later stage of autophagy deficiency–related pathology.

CONCLUSIONS: These results provide the insight that hepatic senescence can occur early in the disease process, triggers inflammation and is enhanced by inflammation, and has long-term effects on liver injury and tumor progression. *(Cell Mol Gastroenterol Hepatol 2022;14:333–355;* https://doi.org/ 10.1016/j.jcmgh.2022.04.003)

Keywords: Chemokines; CCR2; CD11b; CDK Inhibitors; Liver Injury.

S enescence is a cellular status in which cells stop proliferation but remain metabolically active for an extended period. Conversion of normal cells into senescent cells occurs throughout the lifetime of an organism in response to endogenous or exogenous stress signals. Senescence my reflect cellular injury, aging, or loss of function in an autonomous way and can be important in playing a pathologic role while maintaining certain homeostasis in many tissues,[1] including the liver.[2,3] It can occur to hepatocytes in cirrhotic conditions,[4,5] to cholangiocytes in primary biliary cholangitis or in primary sclerosing cholangitis,[6,7] or to stellate cells during fibrosis.[8] However, the triggering molecular mechanisms and pathogenic impact of senescence in liver diseases are not well defined.

Macroautophagy, hereafter referred to as *autophagy*, is an essential biological process of cellular degradation and is widely involved in human pathogenesis.[9,10] Autophagy is important for nutrient regeneration, organelle turnover, clearance of aggregated cellular materials, and defense against intracellular pathogens. Autophagy plays a critical role in hepatic homeostasis.[11–13] Electron microscopic study has found that *Atg7-/-* hepatocytes contain multiple concentric membranous structures, deformed mitochondria, and ubiquitin-positive aggregates.[14] Mice with hepatic autophagy deficiency present with severe hepatomegaly, liver injury, inflammation, fibrosis, and tumorigenesis,[15–19] all pathologic features that are seen commonly in human chronic liver diseases. These features indicate that hepatic autophagy deficiency can be a pathophysiologically relevant model to investigate how senescence can be induced and can contribute to the liver pathology.

Using a mouse genetic model of autophagy deficiency, we have defined senescence as an early onset event soon after the deletion of a key autophagy gene in hepatocytes. Senescence in hepatocytes requires nuclear factor erythroid 2-related factor 2 (NRF2)-mediated events that include oxidative stress, DNA damage, and up-regulation of cyclin-dependent kinase inhibitors (CDKis). The development of senescence-associated secretory phenotype (SASP) correlates with the activation of forkhead box K1 (FOXK1), but not that of nuclear factor-κB (NF-κB), and is regulated by NRF2. A unique feature of autophagy-related SASP is the production of chemokines, instead of inflammatory cytokines, which are responsible for parenchymal inflammation and feedback enhancement of senescence, resulting in a long-term impact on liver injury and tumor progression. This study thus defines how hepatic senescence can be induced and what its pathological impact could be in autophagy deficiency.

Results

Hepatic Autophagy Deficiency Causes Hepatocellular Senescence

Mice with genetic deletion of a key autophagy gene, *Atg7* or *Atg5*, in the liver (*Atg7$^{\Delta Hep}$* or *Atg5$^{\Delta Hep}$*) develop severe liver injury.[15–17] To determine whether senescence was developed under this condition we examined the senescence-associated β-galactosidase (SA–β-gal) activity and the expression of CDKi in the liver.

We found that SA–β-gal activity was significantly induced in approximately 20%–25% of hepatocytes in *Atg7$^{\Delta Hep}$* or *Atg5$^{\Delta Hep}$* livers (Figure 1A and B). Consistently, there was an age-dependent increase of CDKi, *p15/Cdkn2b*, *p21/Cdkn1a*, and *Cdkn3* (Figure 1C and D), but not *p18/Cdkn2c*, *p19/Cdkn2d*, *p27/Cdkn1b*, or *p57/Cdkn1c* (Figure 1E). We also confirmed the increase of p15/CDKN2b and p21/CDKN1a at the protein level in the *Atg7$^{\Delta Hep}$* (Figure 1F and G) or *Atg5$^{\Delta Hep}$* (Figure 1H) livers. To determine the temporal increase of these molecules we used a liver-specific inducible model to delete *Atg7* in adult mice (*Atg7$^{ERT2-Hep}$*), in which *Atg7* deletion is detected on day 5 after induction.[17] A significant increase of CDKi was detected at day 5–10 after induction (Figure 1I), which precedes the increase of liver enzymes at day 15,[18] suggesting that the initiation of senescence can be an early event, independent of detectable liver injury. These findings indicate that the activity of CDK4/6/cyclin D complex and CDK2/cyclin E complex, targets of p15/CDKN2b, p21/CDKN1a, and CDKN3, could be inhibited, to prevent cell-cycle progression through the G1 checkpoint.

We further defined that NRF2 was the major driving force for senescence because co-deletion of *Nrf2* in *Atg7$^{\Delta Hep}$* suppressed most of SA–β-gal activity (Figure 1A). Furthermore, the increase of *p15/Cdkn2b* was inhibited significantly by deletion of *Nrf2* at the messenger RNA (mRNA) and protein levels (Figure 2A–C). However, increase of *p21/Cdkn1a* and *Cdkn3* could not be reversed by simple deletion of Nrf2 (Figure 2A), suggesting that additional factors could be involved in their regulation (see later).
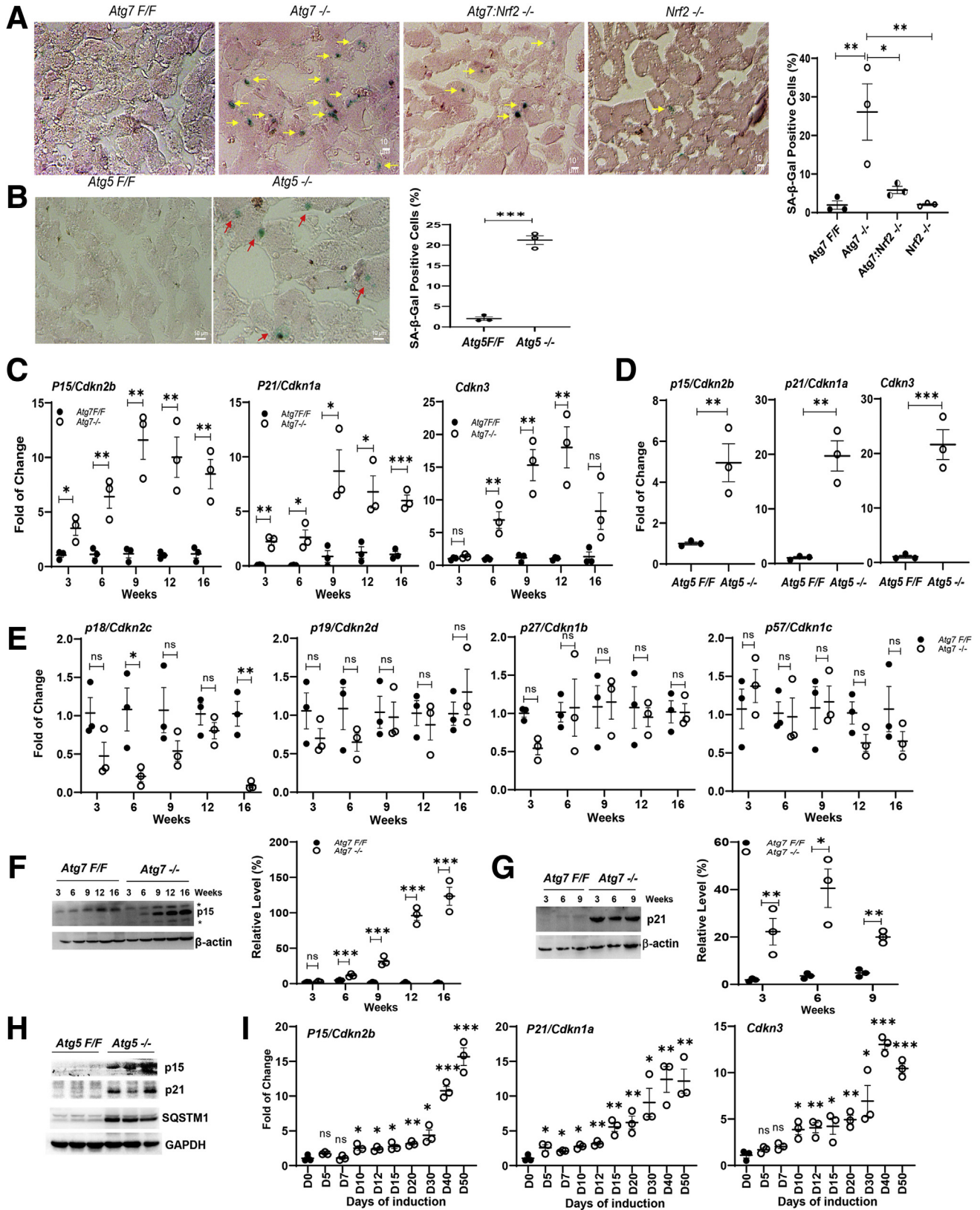
Most current article

Figure 1. Hepatic autophagy-deficiency promotes cellular senescence. (*A* and *B*) Representative images of SA–β-Gal activity in fresh-frozen liver sections of 9-week-old mice of designated genotypes. Blue stains indicate β-galactosidase activity. Positive cells are denoted by *arrows* and quantified. Hepatic mRNA expression of indicated CDK inhibitors in mice of designated genotypes at (*C* and *E*) the indicated ages or at (*D*) 9 weeks old. Immunoblotting analysis of hepatic (*F*) p15/CDKN2b and (*G*) p21/CDKN1a in mice at the indicated age. *Nonspecific bands. *Right*: Quantitative analysis normalized to β-actin. (*H*) Immunoblotting analysis of hepatic (*C*) p15/CDKN2b and (*D*) p21/CDKN1a in 9-week-old mice of designated genotypes. (*I*) mRNA expression of indicated CDK inhibitors was determined in *Atg7$^{Hep-ERT2}$* mice from day 0 to day 50 after tamoxifen treatment. Significance of each group was determined by comparison with day 0. *$P < .05$, **$P < .01$, and ***$P < .001$.
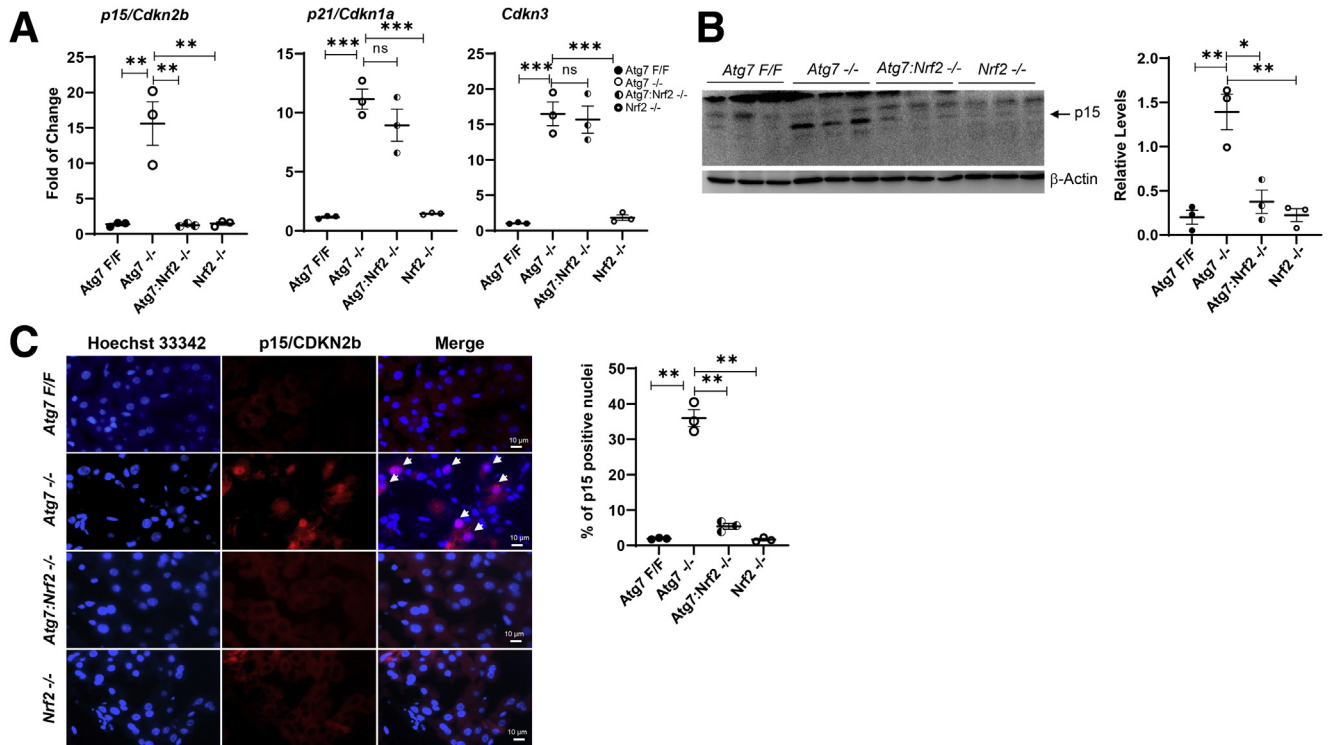
Figure 2. Up-regulation of p15/CKDN2b in autophagy-deficient livers is dependent on NRF2. Expression levels of indicated CDK inhibitors as determined by (*A*) quantitative reverse-transcription PCR, (*B*) immunoblotting, and (*C*) immunofluorescence in 9-week-old mice of designated genotypes. Arrows indicate hepatic nuclei positive for p15/CDKN2b. $*P < .05$, $**P < .01$, $***P < 0.001$.

Hepatocellular Senescence Correlates With DNA Damage and Chromatin Remodeling

Cellular senescence results from the activation of DNA damage response (DDR) and formation of senescence-associated heterochromatic foci (SAHF).[20] SAHF is formed through reorganization of chromatin structure and proliferation-promoting genes are incorporated into transcriptionally silent heterochromatin in senescent cells, and thus unable to be expressed.[21] We detected increased expression of heterochromatic protein 1γ, a known SAHF component,[22] in the autophagy-deficient livers (Figure 3*A*), which was consistent with the formation of SAHF. On the other hand, DDR is thought to impose a permanent cell-cycle checkpoint. DDR is composed of multiple signaling pathways and elements, starting with the DNA damage sensors, which cause phosphorylation and activation of ataxia-telangiectasia mutated (ATM) or ataxia telangiectasia and Rad3-related (ATR), and eventually leads to the activation of downstream kinases and effector molecules.[23] Indeed, we observed that approximately 37% of nuclei in $Atg7^{\Delta Hep}$ livers were phospho--ATM-positive vs 2.7% such positive nuclei in the control $Atg7^{fl/fl}$ livers (Figure 3*B*). H2A histone family member X (H2AX) is phosphorylated by ATM or ATR. The phosphorylated form, known as γ-H2AX, is important for the amplification and sustention of DDR.[20] There was a significantly higher number of γ-H2AX–positive cells in the $Atg7^{\Delta Hep}$ and $Atg5^{\Delta Hep}$ livers (Figure 3*C* and *D*). The number of positive cells accumulated with age (Figure 3*C*).

DDR in autophagy-deficient livers was regulated by NRF2. The increase of both phosphorylated ATM (Figure 3*B*) and γ-H2AX (Figure 3*E*) in $Atg7^{\Delta Hep}$ livers was reduced significantly by the co-deletion of *Nrf2*. However, the increase of nuclear tumor protein p53 (TP53), which is a downstream target of ATM/ATR, in $Atg7^{\Delta Hep}$ livers, but not TP53 acetylation, was reversed by *Nrf2* deletion (Figure 4*A*–*C*), suggesting that the activation of TP53 was regulated by multiple factors. Consistently, neither the up-regulation of *p21/Cdkn1a* (Figure 2*A*) nor that of *Mdm2* (Figure 4*D*), both of which are classic TP53 targets, was reversed by simply co-deleting *Nrf2*.

Along with the DDR, an age-dependent increase of lipid peroxidation was evident in autophagy-deficient livers (Figure 5*A*), which could be reversed by *Nrf2* co-deletion (Figure 5*B*). Because of its low redox potential, the guanine base (G) is most susceptible to oxidation to form 8-oxoguanine (8-oxoG).[24] In autophagy-deficient livers, 80% of cells were found to be 8-oxoG positive and co-deletion of *Nrf2* significantly diminished the presence of 8-oxoG (Figure 5*C*). These results thus supported the model that increased NRF2 activity in autophagy-deficient livers leads to oxidative DNA damage, SASH, and DDR, which promote senescence.

SASP in Autophagy-Deficient Livers Is Characterized by Chemokine Production

SASP is a major feature of senescent cells, which enables the senescent cells to secrete a variety of extracellular
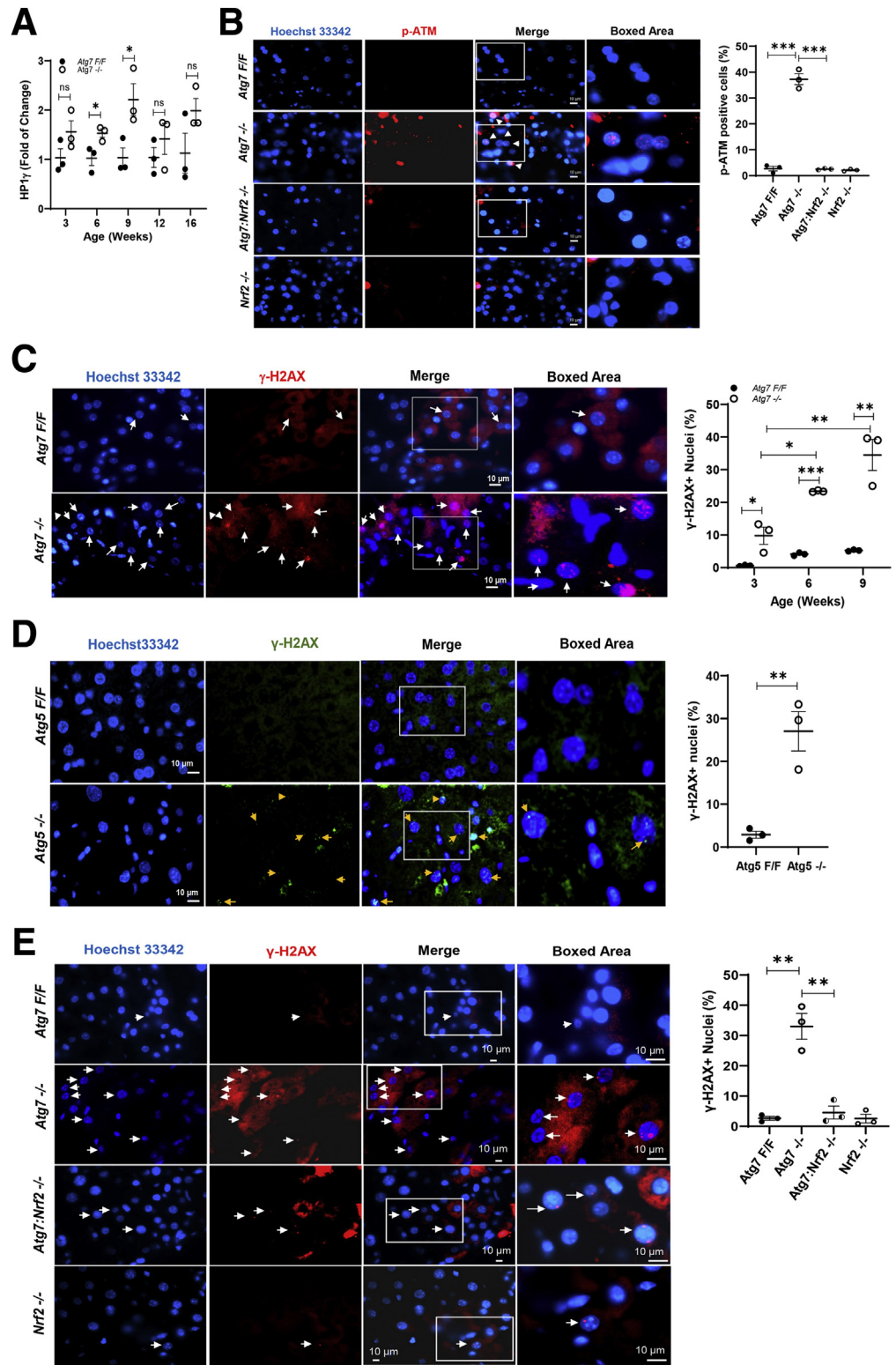
Figure 3. Hepatic autophagy deficiency leads to oxidative DNA damage, DDR, and formation of SAHF. (*A*) Hepatic expression of *HP1*γ in mice of the indicated genotypes and age groups. (*B*) Immunostaining for p-ATM (Ser[1981]) was performed in frozen sections of livers with designated genotypes. p-ATM–positive nuclei are indicated by *arrowheads* and quantified. Liver sections from mice of indicated genotypes and (*C*) indicated ages or (*D* and *E*) at 9 weeks old were immunostained for γ-H2AX. γ-H2AX–positive foci are shown by *arrows* and quantified. *$P < .05$, **$P < .01$, and ***$P < .001$.

modulators that includes cytokines, chemokines, proteases, growth factors, and bioactive lipids.[25] SASP can have a broad impact on cellular environment and disease progression.

We did not see a notable change in the mRNA level of inflammatory cytokines, such as *Il1β*, *Il18*,[17] *Il6*, or *Il4* (Figure 6*A*) in *Atg7*$^{\Delta Hep}$ livers, which are commonly seen in nonhepatic systems.[25] Instead, we detected a robust
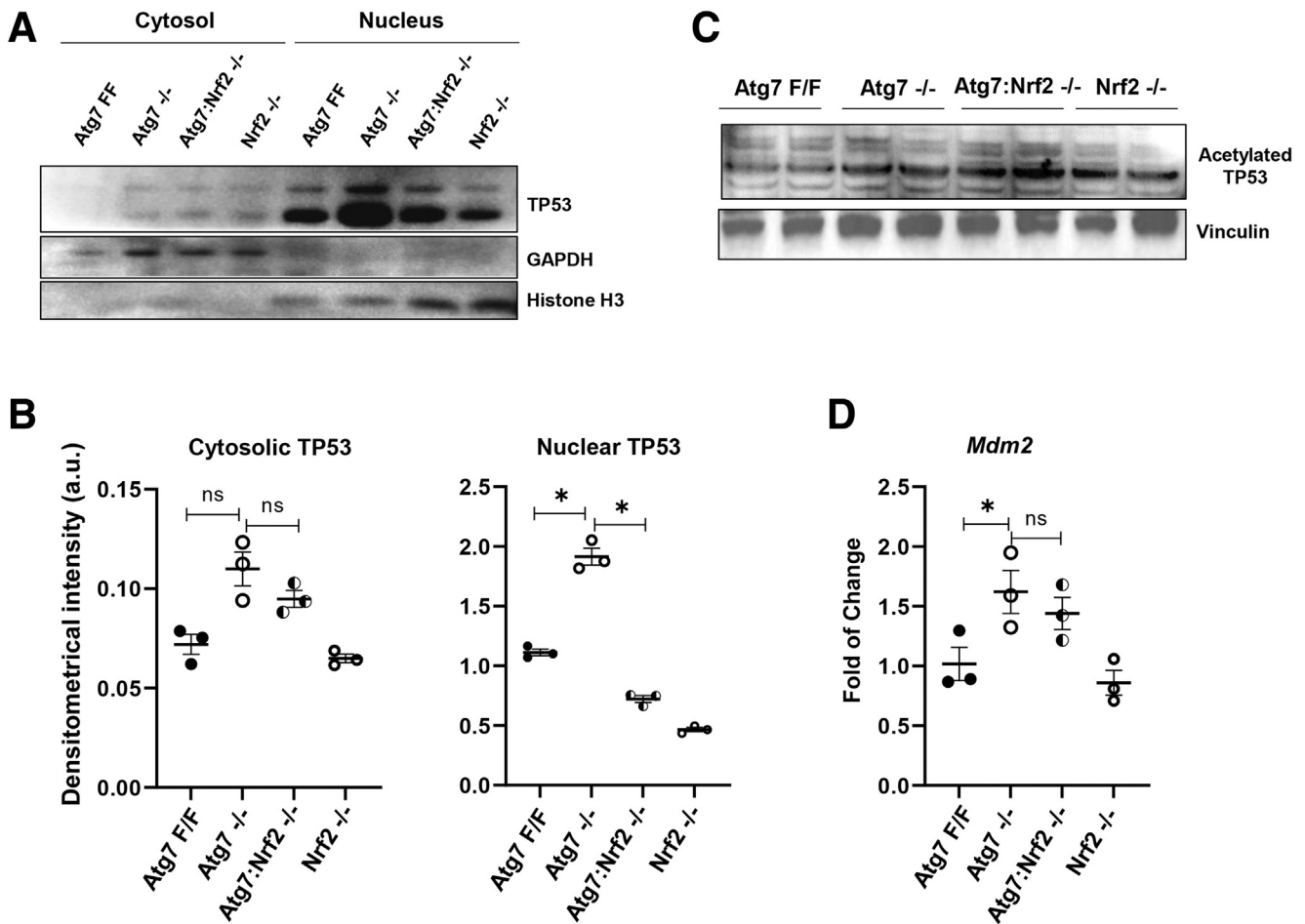
Figure 4. Activation of TP53 could be controlled by both NRF2-dependent and NRF2-independent mechanisms. The cytosolic and nuclear fractions of liver lysates form 9-week-old mice of designated genotypes were (*A*) analyzed by immunoblotting against TP53, and the (*B*) expression levels are quantified by densitometry. (*C*) The total liver lysates form 9-week-old mice of designated genotypes were analyzed by immunoblotting against acetylated TP53. (*D*) The mRNA expression levels of Mdm2 in livers of designated genotypes were quantified by reverse-transcription PCR. *$P < .05$. GAPDH, glyceraldehyde-3-phosphate dehydrogenase.

up-regulation of many chemokine genes, such as *Ccl1*, *Ccl2*, *Ccl7*, *Ccl8*, *Ccl12*, and *Cxcl14* in autophagy-deficient livers (Figure 6*B* and *C*), although down-regulation of some also were observed (Figure 6*D*). We also found significant up-regulation of metalloprotease genes *Mmp12* and *Mmp13*, and type I collagen *Col1a1* in autophagy-deficient livers (Figure 6*E* and *F*). It thus seems that SASP in autophagy-deficient livers could direct a pathologic response of chemotaxis, tissue invasion, and fibrotic repair. In addition, expression of *Tgf-β* also was increased significantly (Figure 6*G*), which also can contribute to senescence.[2] Finally, the increased chemokines depended significantly on the expression of *Nrf2*, as was senescence (Figure 6*H*).

Using C-C motif chemokine ligand 2 (CCL2) as the example, we examined the protein level of this chemokine in the liver and in the serum. The hepatic protein level of CCL2 was decreased significantly in *Atg7*$^{\Delta Hep}$ mice based on both immunoblotting and immunostaining analyses (Figure 7*A* and *B*), which was associated with the increase of blood CCL2 level (Figure 7*C*). The development of SASP is

correlated closely with senescence. Temporal analysis using the inducible *Atg7* deletion model found that the significant increase of *Ccl2*, *Ccl7*, and *Ccl8* occurred at 10 to 15 days after induction (Figure 7*D*), soon after the expression of the CDKi (Figure 1*H*). Immunoblotting analysis indicated that the hepatic CCL2 level became noticeably reduced 7 days after induction (Figure 7*E*), accompanied with a significant increase of CCL2 in blood by day 15 (Figure 7*F*). These findings indicate that intracellular CCL2 was released from hepatocytes to the blood while the transcriptional expression of *Ccl2* was increased to compensate for the need of secretion.

Autophagy-Deficient Hepatocytes Are Responsible for the Senescence Phenotype

To further confirm that hepatocytes were the major source of the chemokines, we isolated hepatocytes and nonhepatocytes in *Atg7*$^{ERT2-Hep}$ mice at day 20, 29, or 100 of the induction of the *Atg7* deletion. The relative purity of the
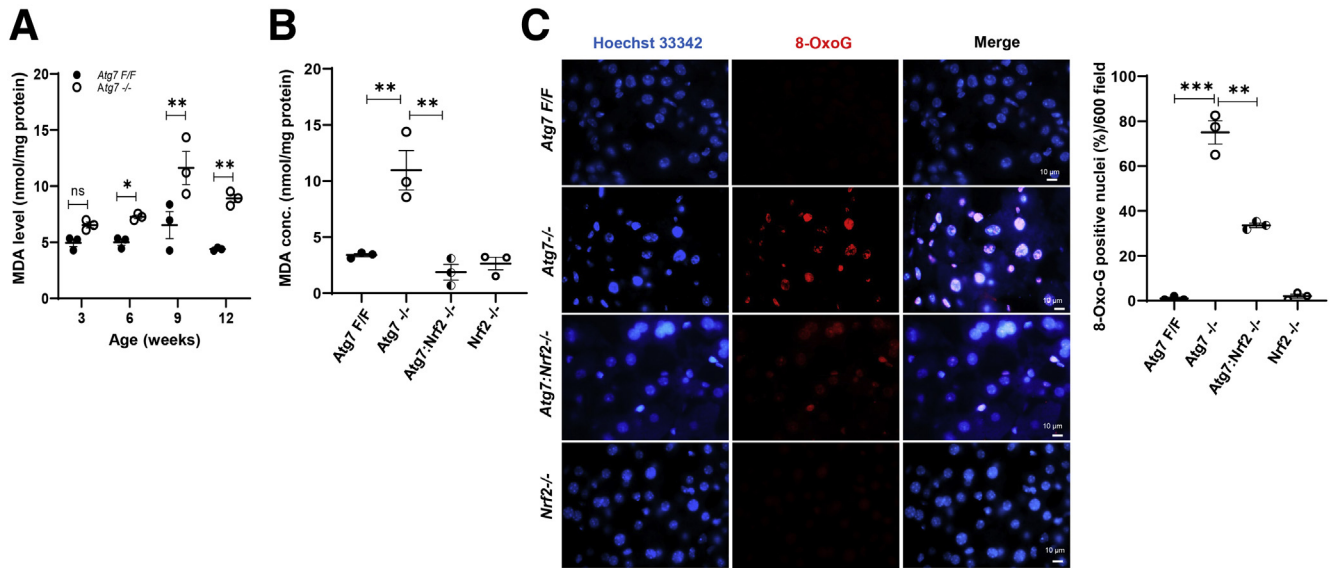
Figure 5. NFR2 regulates oxidative stress and DNA damage in autophagy-deficient livers. (*A* and *B*) The level of malondialdehyde (MDA) in livers of the indicated groups were determined. (*C*) Immunostaining for 8-OxoG in frozen sections of livers of the designated genotypes. Positive nuclei were quantified. All samples were taken from 9-week-old mice unless otherwise indicated. *$P < .05$, **$P < .01$, and ***$P < .001$. conc., concentration.

2 fractions was shown by the differential expression of albumin and α-smooth muscle actin, respectively (Figure 8A). Indeed, it was the hepatocytes that expressed a significantly higher level of *Ccl2*, *Ccl7*, and *Cxcl14*, compared with that in nonparenchymal cells (Figure 8B). Consistently, the significant increase of *p15/Cdkn2b*, *p21/Cdkn1a*, and *Cdkn3* was observed only in isolated *Atg7*-deficient hepatocytes by polymerase chain reaction (PCR) (Figure 8C). Furthermore, isolated hepatocytes also were positive for SA–β-gal activity (Figure 8D).

Noncanonical Regulation of CCL2 Expression in Autophagy-Deficient Livers

SASP is a complex phenotype and could be regulated by different mechanisms in different contexts. NF-κB is known to mediate the transcription of multiple cytokines in various conditions including senescence.[25,26] Activation of NF-κB is characterized by the nuclear translocation of the p65/ Nuclear Factor NF-Kappa-B P65 Subunit (RELA) component of the complex. However, we could not find any significant difference in the nuclear level of p65/RELA between *Atg7$^{\Delta Hep}$* and *Atg7$^{fl/fl}$* livers via immunoblotting and immunofluorescence staining (Figure 9A–C). In addition, the mRNA expression of *p65/RelA*, *p50/NF-κB1*, and *p52/NF-κB2* were not up-regulated in autophagy-deficient livers (Figure 9D). Moreover, we could not detect NF-κB transcriptional activity in the nuclear fraction of *Atg7$^{\Delta Hep}$* and *Atg7$^{fl/fl}$* mouse livers (Figure 9E). These data suggest that the NF-κB pathway may not be involved in SASP in autophagy-deficient livers.

Another transcription factor, GATA binding protein 4 (GATA4), recently was found to be a senescence and SASP regulator.[27] The GATA4 protein level was increased in the liver of older mice, but with no apparent differences between *Atg7$^{fl/fl}$* and *Atg7$^{\Delta Hep}$* mice (Figure 10A). In addition, there was no apparent nuclear translocation of GATA4 (Figure 10B), and the mRNA expression of *Gata4* and its target gene, *Traf3ip2*, was not up-regulated but down-regulated in autophagy deficiency (Figure 10C), suggesting that the GATA4 pathway was not activated.

FOXK1 recently was found to be activated by protein phosphatase 2A (PP2A) through dephosphorylation, and in turn transcriptionally activates *Ccl2* expression in cancer cells independently of NF-κB signaling.[28] We found that the level of FOXK1 was mildly reduced in *Atg7$^{\Delta Hep}$* livers, but all 3 subunits of PP2A were increased significantly in total lysates (Figure 11A and B) and in the nucleus (Figure 11C). Nuclear FOXK1 is dephosphorylated by PP2A. Consistently, the nuclear level of phosphorylated FOXK1 was reduced in autophagy-deficient livers (Figure 11D and E). Notably, FOXK1 dephosphorylation depended on NRF2 so that the nuclear level of phosphorylated FOXK1 was reversed in *Atg7*-deficient hepatocytes with co-deletion of *Nrf2* (Figure 11E). Overall, our data suggest that FOXK1 is activated and can be involved in the regulation of CCL2 expression in the autophagy-deficient liver.

Ccr2 Deletion Reduces Inflammation in Autophagy-Deficient Livers

Deletion of *Atg7* or *Atg5* in the liver not only caused liver injury, but also inflammation, as shown by increase of F4/80^{+17} or CD11b$^+$ macrophages (Figure 12A–C). In the *Atg7$^{\Delta Hep}$* liver, we also found that this inflammation was mediated by NRF2-dependent mechanism because co-deletion of *Nrf2* significantly reduced parenchymal infiltration by inflammatory cells (Figure 12A and B).
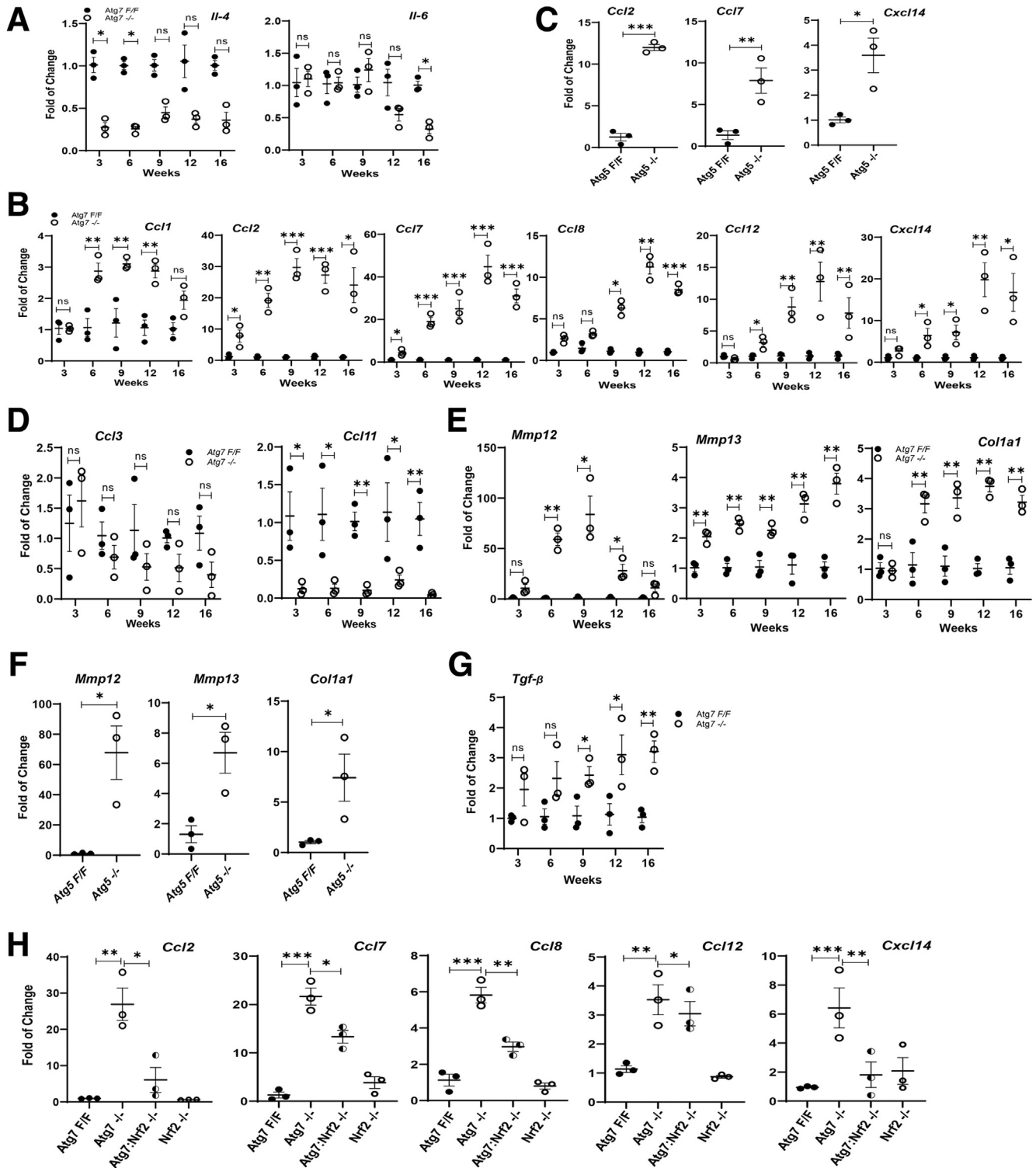
Figure 6. Hepatic autophagy deficiency induces SASP in a NRF2-dependent way. The hepatic mRNA levels of the indicated cytokine genes or chemokine genes were quantified in (*A, B, D, E, G*) 3- to 16-week-old *Atg7 F/F* and *Atg7^{ΔHep}* (*Atg7-/-*) mice or in (*C* and *F*) 9-week-old *Atg5 F/F* and *Atg5^{ΔHep}* (*Atg5-/-*) mice. (*H*) Hepatic mRNA expression of the indicated chemokines in 9-week-old mice of the designated genotypes. *$P < .05$, **$P < .01$, and ***$P < .001$; *Atg7-/-* or *Atg5-/-* vs the respective floxed mice or as indicated.
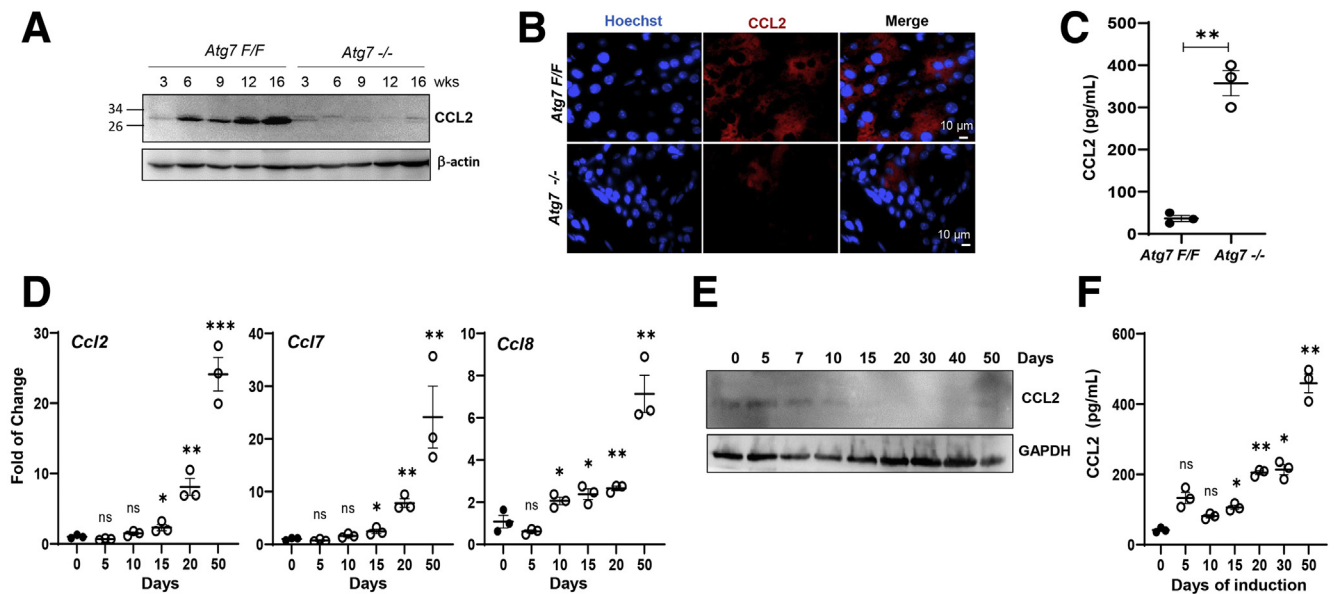
Figure 7. Reduction of CCL2 in the liver is correlated with an increase in the serum in Atg7-deficient mice. (*A*) Hepatic protein levels of CCL2 in mice of the indicated age and genotype groups. (*B*) Immunofluorescence staining for CCL2 in the liver of 9-week-old mice of indicated genotypes. (*C*) Serum level of CCL2 in 9-week-old mice of the indicated genotypes. (*D*) The hepatic mRNA expression of the indicated chemokines was determined in $Atg7^{Hep-ERT2}$ mice on different days after tamoxifen treatment. Significance was compared with day 0. (*E*) Hepatic and (*F*) serum levels of CCL2 in $Atg7^{Hep-ERT2}$ mice on day 0 to day 50 after tamoxifen treatment. $*P < .05$, $**P < .01$, and $***P < .001$. GAPDH, glyceraldehyde-3-phosphate dehydrogenase.

Because CCL2 family chemokines were highly up-regulated in a NRF2-dependent fashion in autophagy deficiency we reasoned that chemokine-mediated recruitment of inflammatory cells was responsible for the parenchymal inflammation. We thus deleted the gene *Ccr2* in $Atg7^{\Delta Hep}$ mice. CCL2 encodes the receptor that can interact with CCL2, CCL7, and CCL12 in mice,[29] and is highly expressed by monocytes[30] and T cells.[31] Indeed, deletion of *Ccr2* significantly reduced CD11b$^+$ cells in the *Atg7*-deficient livers (Figure 12*A* and *B*). In addition, an increase of CD3$^+$ cells, but not CD45R$^+$ cells, was observed in *Atg7*-deficient livers,[17] which also was suppressed by *Ccr2* deletion (Figure 12*D* and *E*). Inflammation seemed to increase over time because the number of parenchymal CD11b$^+$ cells was higher in older mice at the ages of 9 and 12 months (Figure 12*F* and *G*) compared with that in the 9-week-old mice (Figure 12*B*), but still largely was regulated by C-C motif chemokine receptor 2 (CCR2)-mediated events.

Ccr2 Enhances Senescence and SASP in Autophagy-Deficient Livers

In young mice at the age of 9 weeks, deletion of *Ccr2* also significantly reduced the SA–β-gal activity in $Atg7^{\Delta Hep}$ livers (Figure 13*A*), along with a significantly reduced γ-H2AX foci positivity (Figure 13*B*), and a significantly reduced expression of *p21/Cdkn1a* and *Cdkn3* (Figure 13*C*). Reduction of *p15/Cdkn2b* also was noted, although the change was not significant. Furthermore, the expression of several chemokines, *Ccl2*, *Ccl7*, *Cxcl14*, as well as *Tgf-β*, was significantly reduced in the $Atg7^{\Delta Hep}:Ccr2^{-/-}$ livers, compared with that in the $Atg7^{\Delta Hep}$ livers (Figure 13*D*). Transforming growth factor-β could

enhance senescence via p15/CDKN2b[32] or p21/CDKN1[7] in a paracrine mode. These observations suggested that CCR2-mediated inflammation could positively enhance hepatocyte senescence and SASP, which could enhance inflammation further, mainly through the p21/CDKN1a, CDKN3, and transforming growth factor-β–mediated mechanisms. In contrast, neither the ductular reaction, as shown by SRY (Sex-Determining Region Y)-Box 9 Protein (SOX9) staining and quantification (Figure 14*A* and *B*) or by H&E staining (Figure 14*C*), nor the fibrotic response (Figure 14*D* and *E*), was reduced by the deletion of *Ccr2* in $Atg7^{\Delta Hep}$ mice.

Ccr2 Deletion Affects Hepatomegaly, Liver Injury, and Tumorigenesis

Although CCR2 was important for hepatic inflammation in both young and old $Atg7^{\Delta Hep}$ mice, the impact on liver injury was noted mainly in mice at the age of 9 months so that deletion of *Ccr2* significantly reduced hepatomegaly and serum levels of liver enzymes (Figure 15*A*). Such effects were not prominent across the different parameters in other age groups (Figure 15*B* and *C*). Coincidently, tumor development in the 9-month-old $Atg7\Delta Hep:Ccr2^{-/-}$ mice was delayed significantly compared with that in $Atg7^{\Delta Hep}$ mice, as measured by the tumor burden and the size (Figure 16*A* and *B*). In addition, mRNA expression levels of the oncofetal genes *Afp*, *Igf2*, and *Rex3* also were decreased in $Atg7^{\Delta Hep}:Ccr2^{-/-}$ livers (Figure 16*C*).

However, by age 12 months, tumor development in $Atg7^{\Delta Hep}:Ccr2^{-/-}$ livers became comparable with that in the $Atg7^{\Delta Hep}$ livers in terms of tumor numbers per mouse (Figure 16*D*), although the double-knockout livers tended to
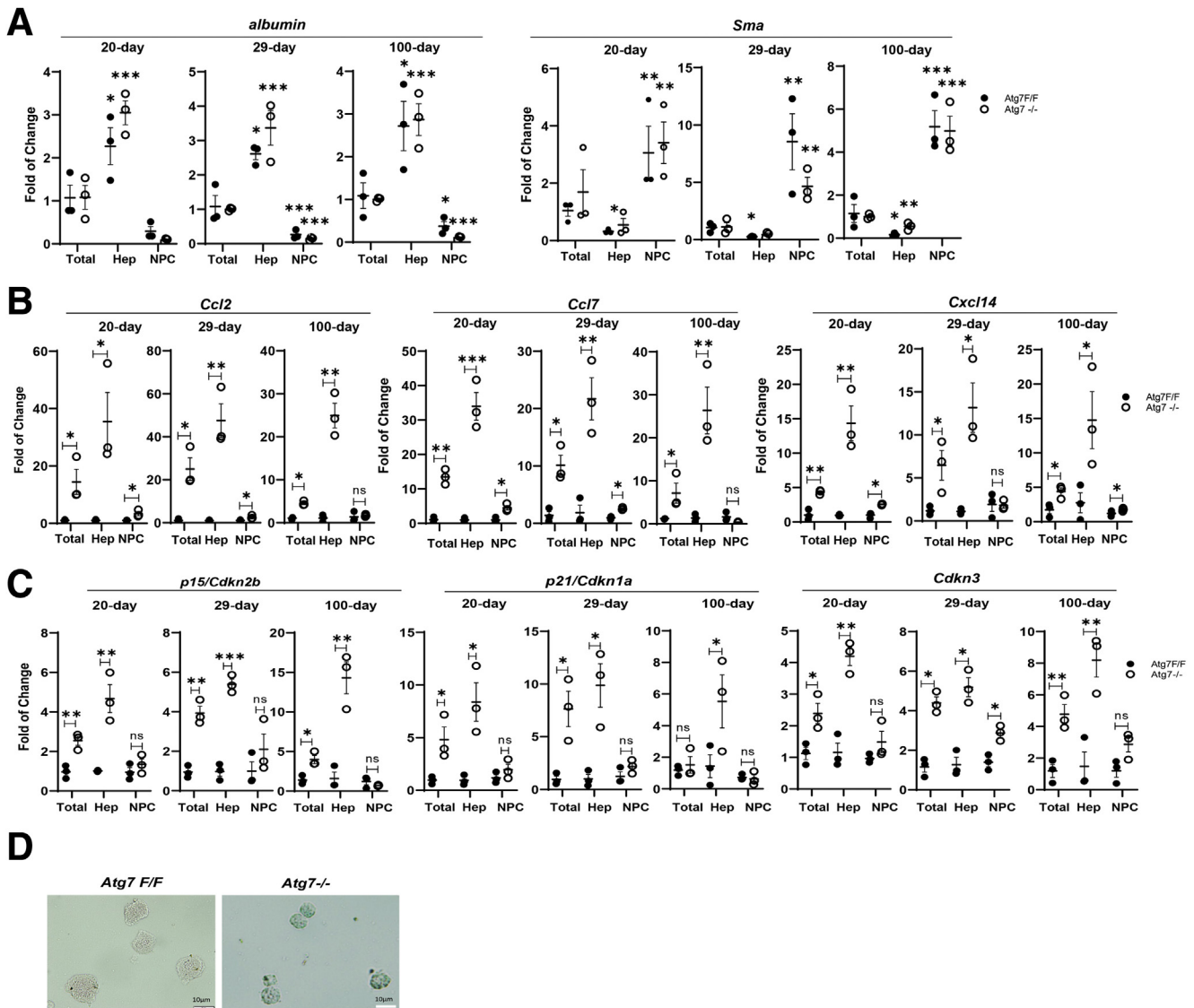
Figure 8. Assessment of the senescence and chemokine expression in isolated hepatocytes and nonparenchymal cells. (*A*) The mRNA levels of albumin and smooth muscle actin (*sma*) in the total liver cells (Total), and in separated hepatocytes (Hep) or nonparenchymal cells (NPC) from the livers of *Atg7^Hep-ERT2* mice on days 20, 29, and 100 after tamoxifen treatment (*Atg7-/-*) and from the livers of nontreated *Atg7^Hep-ERT2* mice (*Atg7 F/F*). The mRNA levels (*B*) of selected chemokines and (*C*) cell-cycle inhibitors in the total liver cells, and in separated hepatocytes or nonparenchymal cells from *Atg7^Hep-ERT2* mice on days 20, 29, and 100 after tamoxifen treatment (*Atg7-/-*) and from the livers of noninduced *Atg7^Hep-ERT2* mice (*Atg7+/+*). (*D*) Representative images of SA–β-Gal activity in fresh hepatocytes isolated from *Atg7^Hep-ERT2* mice without induction (*Atg7 F/F*) or with indication at day 100 of tamoxifen treatment (*Atg7-/-*). Blue stains indicate β-galactosidase activity. *P < .05, **P < .01, and ***P < .001; *Atg7-/-* vs *Atg7 F/F* for each cell category.

have smaller tumors (Figure 16*E*). Histologically, there did not seem to be a noticeable difference in the morphology of tumors derived from the *Atg7^ΔHep* livers and *Atg7^ΔHep:Ccr2^-/-* livers (Figure 16*F*). Tumors in both cases seemed to be benign with a clear border. Finally, *Afp* and *Igf2* also were expressed at similar levels (Figure 16*G*). These observations indicate that chemokine–CCR2 interaction affects tumor development in autophagy-deficient livers at the relatively early stage of tumorigenesis when the tumors became grossly detectable, which is similar to the regulation by high mobility group box 1 (HMGB1) and receptor for advanced glycation end products.[17,33]

Discussion

Although senescence is readily observable in livers with chronic injuries, its contribution to liver pathology is not as clear.[2–6,8] Direct induction of senescence through genetic manipulations, such as deletion of *Mdm2* in hepatocyte or cholangiocytes, provides direct evidence that hepatic senescence has pathologic consequences.[2,7] Studies using a more physiologically relevant model are limited in terms of linking senescence to other pathology changes.

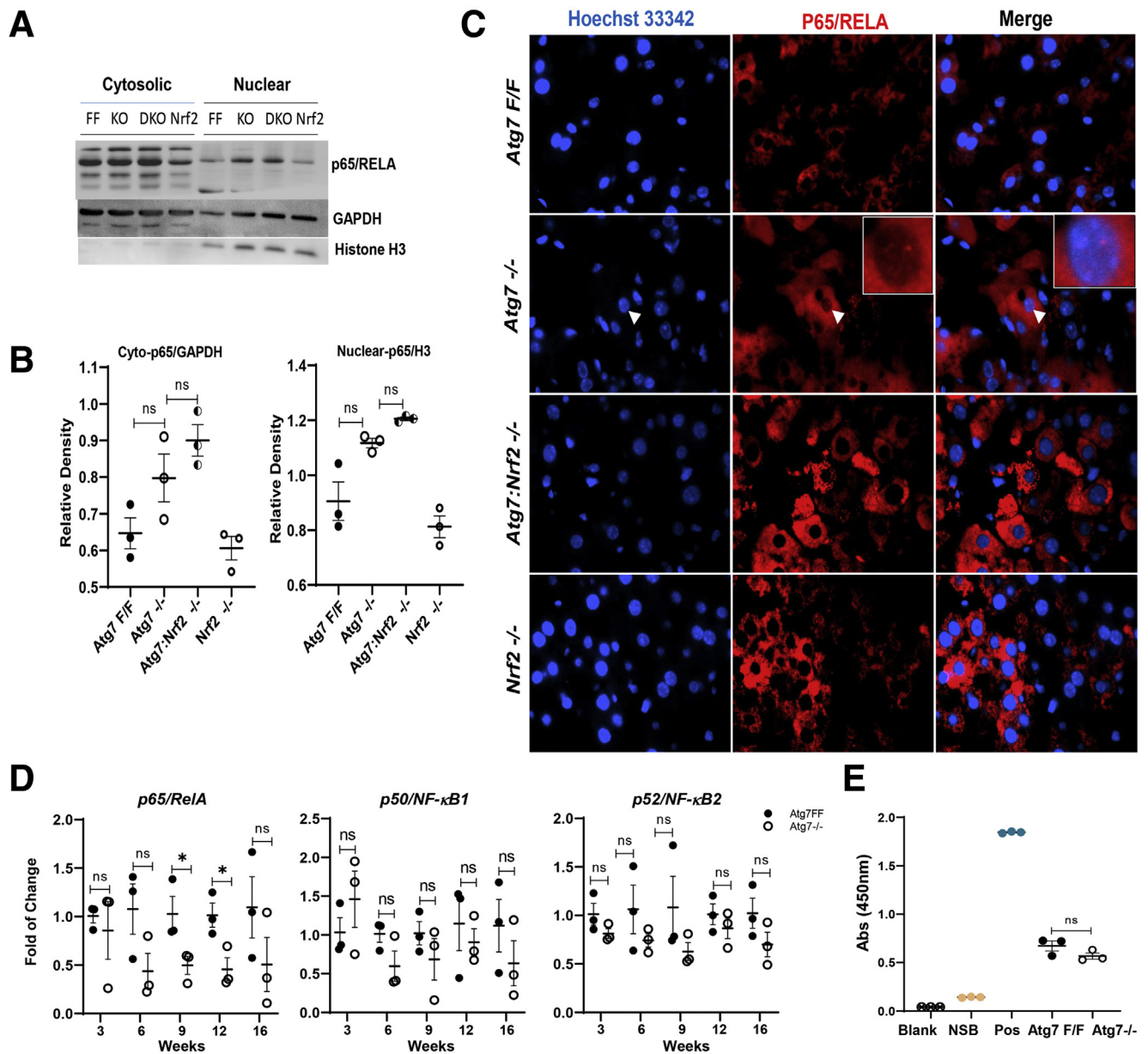Autophagy and senescence are known to be mutually affected in nonhepatocytes in different context.[34–36] In

Figure 9. The NF-κB pathway is not activated in autophagy-deficient livers. (*A*) The hepatic cytosolic and nuclear level of p65/RELA in *Atg7 F/F* (*FF*), *Atg7-/-* (*KO*), *Atg7:Nrf2-/-* (*DKO*), and *Nrf2-/-* (*Nrf2*) mice. (*B*) The cytosolic and nuclear levels of hepatic p65/RELA were quantified by densitometry and normalized to the level of glyceraldehyde-3-phosphate dehydrogenase (GAPDH) and H3 histone, respectively. (*C*) Immunostaining for p65/RELA was performed on fresh-frozen liver sections from 9-week-old mice of designated genotypes. *Arrowheads* indicate 1 cell in which nuclear p65/RELA could be observed. (*D*) The hepatic mRNA levels of *p65/RelA*, *p50/NF-κB1*, and *p52/NF-κB2* genes were quantified in 9-week-old mice. (*E*) The nuclear NF-κB transcriptional activity assay was determined in the liver of 9-week-old mice by an enzyme-linked immunosorbent assay (ELISA). Blank, buffer only; NSB, nonspecific binding control (provided by the assay kit); Pos, positive control provided by the kit manufacturer. *$P < .05$; *Atg7-/-* vs *Atg7 F/F*.

human fibroblasts, 1 study showed that senescence could induce autophagy, which in turn promoted senescence,[34] but another study showed that knockdown of autophagy genes caused senescence.[35] Similar to the later, muscle stem cells could maintain a reversible quiescence state and autophagy suppressed senescence.[36] The present study, by disabling autophagy, shows that senescence can occur early in the pathogenesis without a chronic course, and can have a long-term impact on liver inflammation, liver injury, and tumor development. In addition, our study indicates that senescence in autophagy-deficient livers is unique, involving NRF2-mediated oxidative DNA damage and up-regulation of p15/CDKN2b for senescence induction, involving FOXK1 instead of the classic NF-κB pathway for SASP, and involving chemokines instead of inflammatory cytokines for pathology outcomes.
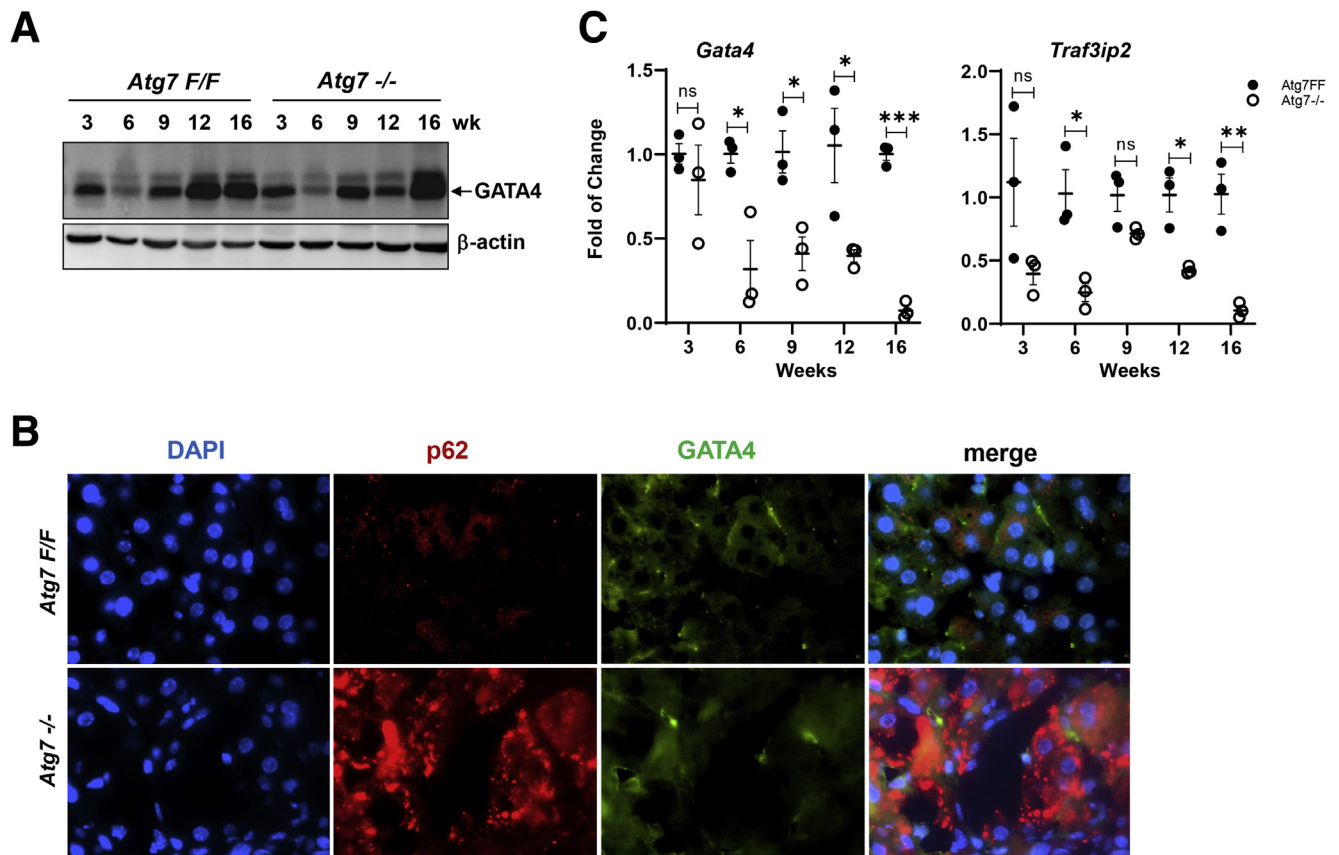
Figure 10. GATA4 is not activated in the autophagy-deficient livers. (*A*) Immunoblotting analysis of hepatic GATA4 in 9-week-old mice. β-actin was used as a loading control. (*B*) Immunostaining of GATA4 was performed in fresh-frozen liver sections from 9-week-old mice. (*C*) The hepatic mRNA levels of *GATA4* and *Traf3ip2* genes were quantified in 9-week-old mice. *$P < .05$, **$P < .01$, and ***$P < .01$. DAPI, 4',6-diamidino-2-phenylindole.

Senescence in Autophagy-Deficient Livers Is an Early Event and Can Be Mediated by Several Intertwined Mechanisms

Hepatic autophagy deficiency relies on several mechanisms to induce senescence. Sustained NRF2 activation is responsible for the oxidative stress, DNA damage, and DDR. We observed the activation of ATM and TP53. There were significant up-regulations of CDK inhibitors p15/CDKN2b, p21/CDKN1a, and CDKN3, which suppress CDK4/cyclin D, CDK6/cyclin D, and/or CDK2/cyclin E complex. Expression of *p16/Cdkn2a*, another well-known CDK inhibitor,[37] was not observed in autophagy-deficient livers using 4 different sets of primers (Table 1).[38] p15/CDKN2b and p16/CDKN2a are the homologs and can functionally compensate each other.[2,32] The expression of *p15/Cdkn2b* can be regulated by NRF2, suggesting that the pathway by *p15/Cdkn2b*-mediated mechanism plays a larger role in the initiation of senescence because the senescent cells and SASP are both greatly reduced in the absence of NRF2.

Notably, unlike *p15/Cdkn2b*, the expression of *p21/Cdkn1a* and *Cdkn3* could not be suppressed by simple deletion of *Nrf2*. However, when the inflammation is suppressed via the deletion of *Ccr2*, hepatic senescence and expression levels of *p21/Cdkn1a* and *Cdkn3*, but not that of

p15/Cdkn2b, were reduced significantly, suggesting that the senescence effect of *p21/Cdkn1a* and *Cdkn3* could be mainly regulated by inflammation in an amplification loop (Figure 17*A*). Further evidence to support this hypothesis may have to be furnished in future studies by constructing mutant mice harboring both autophagy deficiency and *p15/Cdkn2b* or *p21/Cdkn1a* or *Cdkn3* deletion to assess the individual contribution of the different pathways to senescence, SASP, and inflammation. Nonetheless, these mechanisms likely are intertwined and connected to each other (eg, by the SASP-driven inflammation process) in the context of autophagy deficiency.

Senescence in the liver often is seen in the condition of chronic injury,[2,3] but it can be an early event as indicated in the present study. The up-regulation of CDK inhibitors (Figure 1*I*) is earlier in kinetics than the increase of liver enzyme levels in the blood,[18] suggesting that the initiation of senescence can be independent of injury. This finding also may suggest that the role of NRF2 in senescence is independent of its role in injury, although this possibility cannot be completely ruled out. Thus, NRF2 may regulate senescence in parallel with, or independent of, its involvement in the development of liver injury. NRF2 also is known to be involved in the regulation of senescence in many other
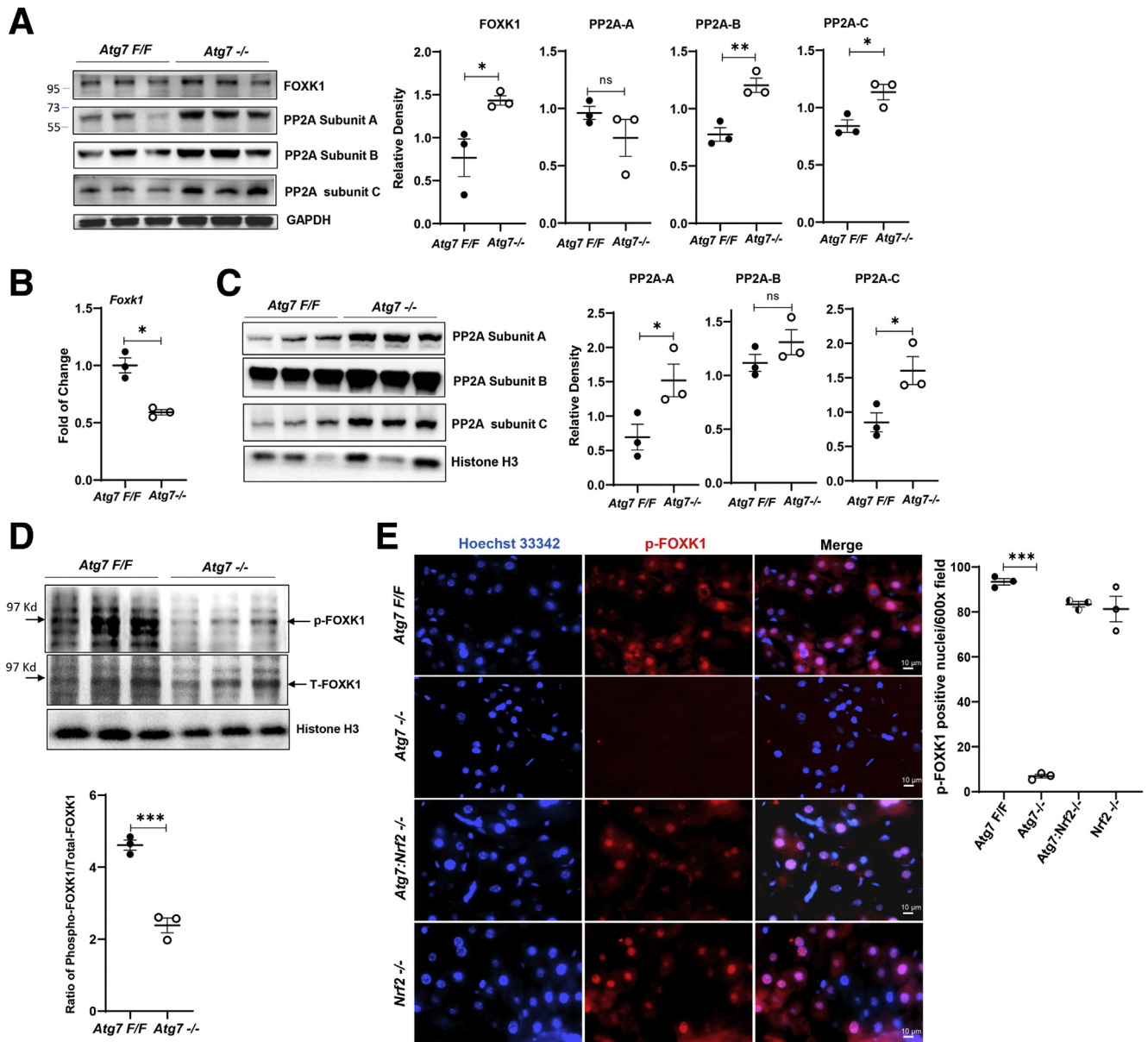
Figure 11. Down-regulation of nuclear phospho-FOXK1 in Atg7^{ΔHep} livers. (A) Immunoblotting and densitometry analysis of FOXK1 and PP2A subunits in the liver of 9-week-old mice of the designated genotypes. (B) mRNA level of *Foxk1* in the livers of 9-week-old mice. (C) Immunoblotting and densitometry analysis of PP2A subunit A, B, and C in the nuclear fraction of the liver lysates from 9-week-old mice. (D) Immunoblotting and densitometry assay of phosphorylated FOXK1 (p-FOXK1) and total FOXK1 (T-FOXK1) in the liver lysate of 9-week-old mice. (E) Liver sections from 9-week-old mice of the indicated genotypes were immunostained for p-FOXK1. Nuclei positive for p-FOXK1 were quantified. *$P < .05$, **$P < .01$, and ***$P < .001$. GAPDH, glyceraldehyde-3-phosphate dehydrogenase.

contexts that are not necessarily in response to tissue injury,[39] further supporting its independent and direct role in senescence regulation.

SASP in Autophagy-Deficient Livers Triggers Mutual Amplifications of Inflammation and Senescence

The impact of senescence is not limited to the cells undergoing this process, but can be on other cells through SASP, thus having a broad effect. The profile of SASP can vary in different contexts, which leads to different outcomes. SASP manifested in autophagy-deficient livers is unique because there is no up-regulation of the classic inflammatory cytokines including interleukin (IL)1β, IL18, IL6, or tumor necrosis factor α. In contrast, the SASP is represented by the robust production of a variety of chemokines, particularly the CCL2 family chemokines, which bind to a common receptor: CCR2.[29] The unique features of the autophagy-related hepatic SASP is reflected in both the
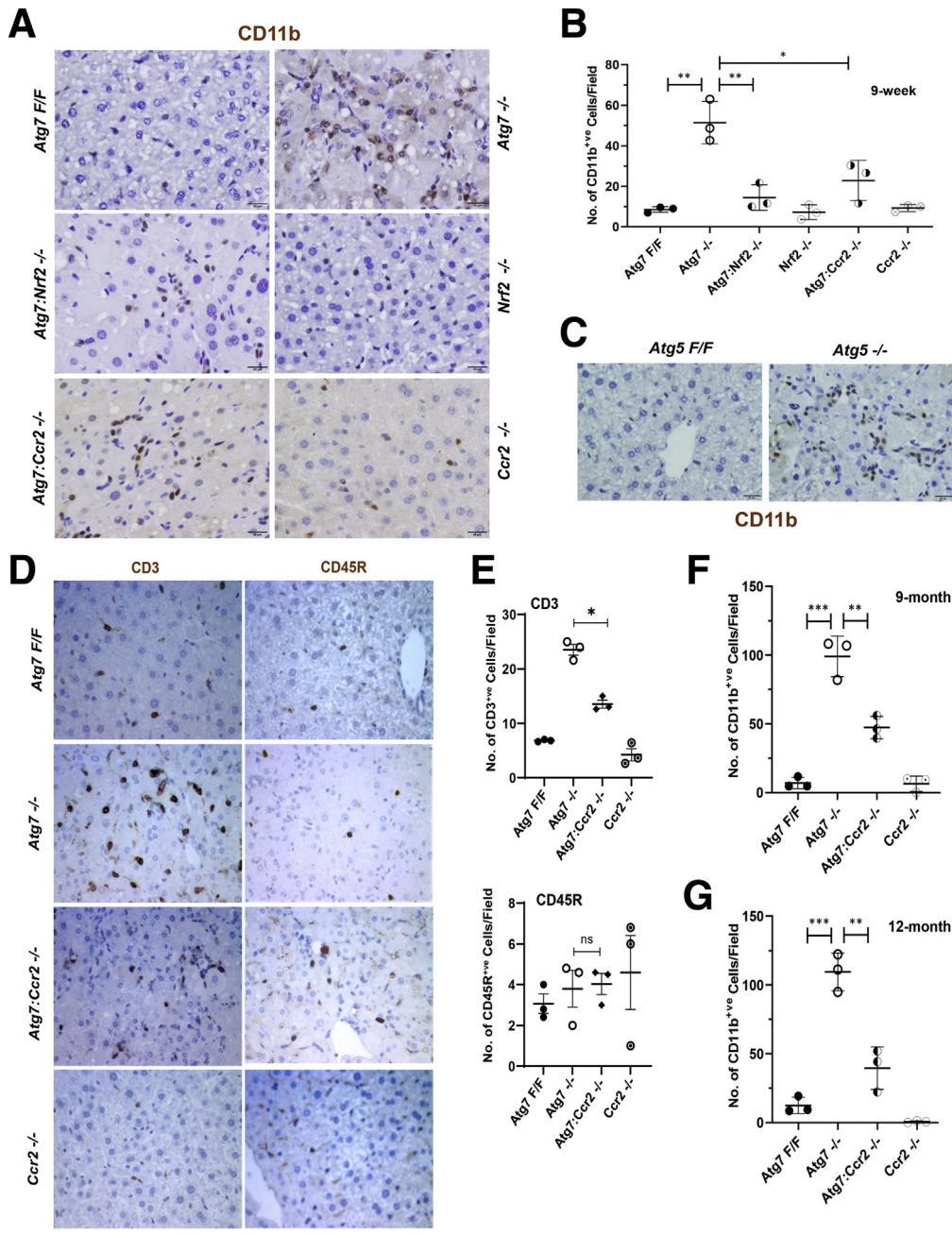
Figure 12. Deletion of *Ccr2* gene in autophagy-deficient livers reduces parenchymal inflammation. Liver sections of 9-week-old mice with designated genotypes were subjected to (*A* and *C*) anti-CD11b staining, and (*D*) anti-CD3 or anti-CD45 staining. (*B* and *E*) Positive cells were quantified per field (original magnification, ×400). Liver sections of (*F*) 9-month-old or (*G*) 12-month-old mice with designated genotypes were subjected to anti-CD11b staining. Positive cells were quantified per field (original magnification, ×400). *P < .05, **P < .01, and ***P < .001.

mechanisms and the outcomes. Notably, we have not observed the activation of NF-κB, which frequently is associated with SASP in nonhepatocytes and a main regulator of the expression of inflammatory cytokines.[25] Similarly, it does not seem that the GATA4 pathway, which has been noted in nonhepatocytes,[27] is involved in the present case.

CCL2 is a representative chemokine, and it recently was shown that its up-regulation could be mediated by a novel non–NF-κB pathway involving FOXK1.[28] Indeed, we found that FOXK1 is activated in a dephosphorylated form in autophagy-deficient hepatocytes in a NRF2-dependent manner. The expression of all 3 components of PP2A was

increased, which are responsible for the dephosphorylation of FOXK1.[28] Thus, it seems that activation of chemokines in the autophagy-deficient livers depends on a non–NF-κB pathway involving FOXK1.

Together with our early finding that signaling of HMGB1, a pattern recognition molecule often associated with inflammation, and the inflammasome, are dispensable for inflammation induction in autophagy-deficient livers.[17] The much more robust expression of chemokines over that of inflammatory cytokines indicates that the parenchymal inflammation is contributed mainly by the recruitment of extrahepatic CD11b$^+$ monocytes and CD3$^+$ T cells.
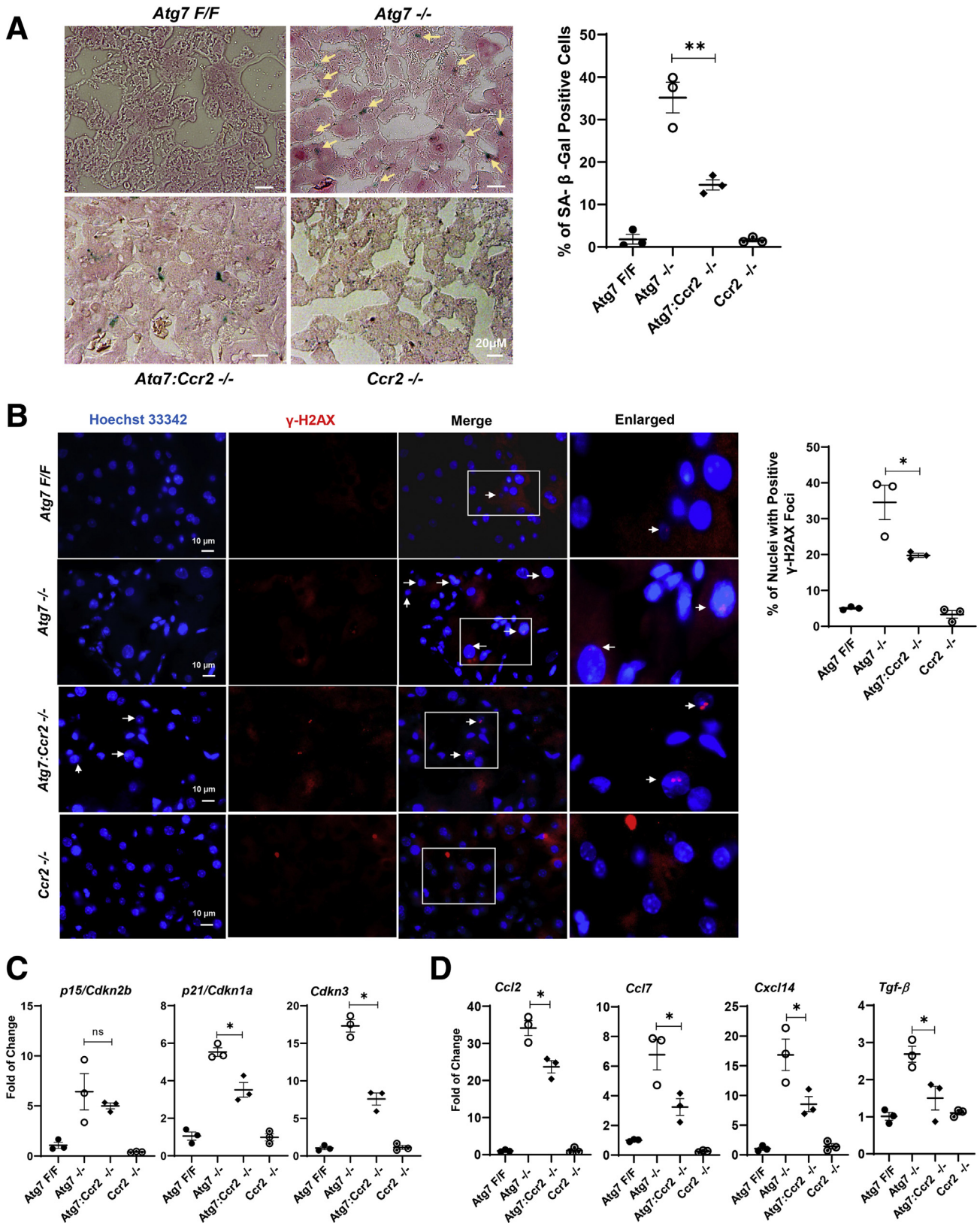
Figure 13. Deletion of *Ccr2* gene in autophagy-deficient livers reduces hepatic senescence. (*A*) Representative images showing SA–β-Gal activity in fresh-frozen liver sections of 9-week-old mice of the designated genotypes. Cells with blue staining were quantified as SA–β-Gal–positive cells. (*B*) γ-H2AX–positive nucleus were quantified in liver sections from 9-week-old mice of the designated genotypes. (*C and D*) The hepatic mRNA levels of the indicated genes were quantified in 9-week-old mice of the designated genotypes. *$P < .05$, **$P < .01$.
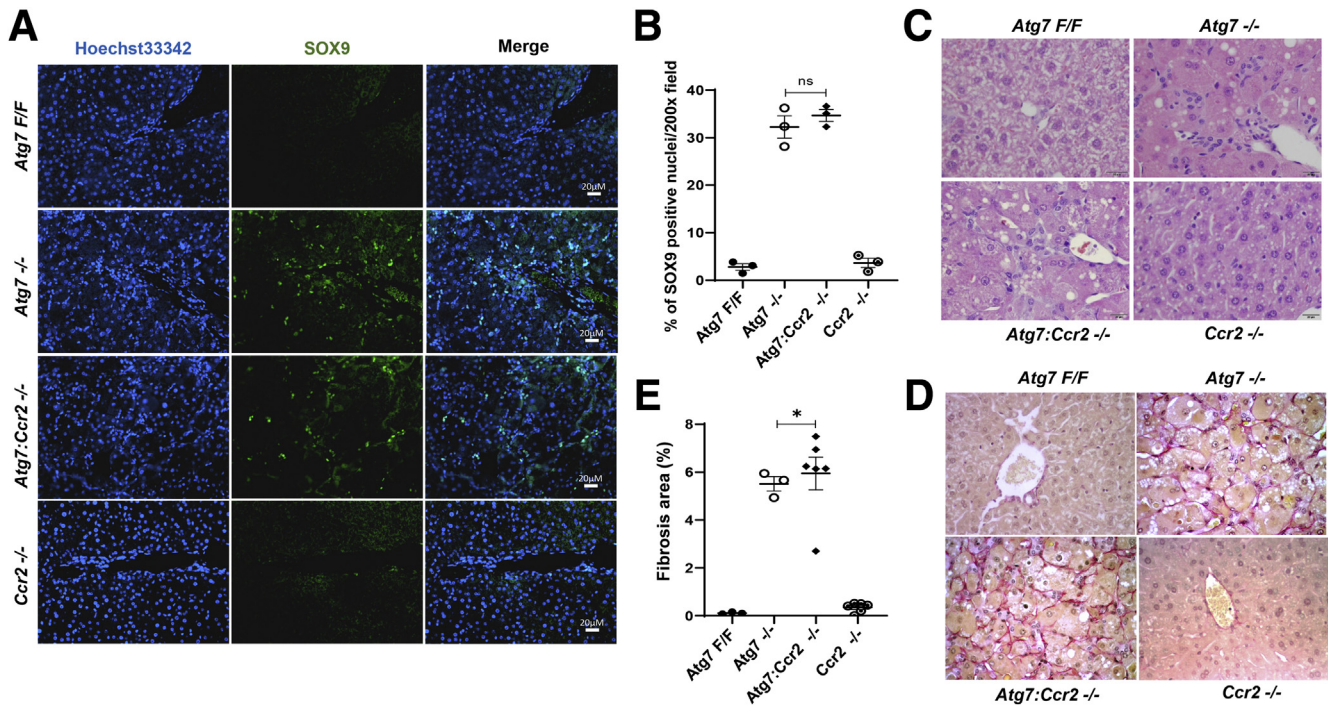
Figure 14. Deletion of the *Ccr2* gene does not affect the ductular response and fibrosis in autophagy-deficient livers. Liver sections from 9-week-old mice of the designated genotypes were immunostained for (*A*) SRY (Sex-Determining Region Y)-Box 9 Protein (SOX9), and (*B*) SOX9–positive cells were quantified. Liver sections from mice of different genotypes were stained with (*C*) H&E or (*D*) Sirius Red (original magnification, ×400). (*E*). The fibrotic area in panel *C* is quantified. *$P < .05$.

Surprisingly, deletion of *Ccr2* not only inhibits the inflammation, but also reduces senescence and chemokine production. Thus, in autophagy-deficient livers, senescence and inflammation mutually enhance each other in an amplification loop (Figure 17*B*).

Autophagy Deficiency Can Affect Tumor Progression Extrinsically via CCR2-Mediated Inflammation

Autophagy is an evolutionarily conserved mechanism that can provide surveillance functions on tumor development. By removing cell-damaging degenerative organelles or protein aggregates, autophagy can mitigate various stress signaling pathways that promote tumorigenesis.[40] Thus, deficiency in autophagy function can render the cell prone to tumor development as seen in the liver models used here.[15–17] Paradoxically, for many types of cancers, particularly those driven by the Ras mutation, intrinsic autophagy function also is required for aggressive growth by providing metabolic support.[41] Thus, cancers derived from loss of autophagy function tend to develop less aggressively than those with intact autophagy function.[40] Nevertheless, these tumors may depend on other context-related extrinsic factors for growth. For example, in an early study we showed that autophagy-deficient hepatocytes release HMGB1, which promotes tumor progression.[17]

In this study we have defined another extrinsic mechanism: senescence-driven inflammation that can promote the progression of autophagy-deficient tumors. Neither the HMGB1-mediated mechanism nor the CCR2-mediated mechanism is absolutely required for tumor development because the deletion of either will not stop the tumor from occurring, but both can delay the occurrence of gross tumor significantly. Thus, they do not seem to act at the initiation step, but at the progression stage. Another common feature of the HMGB1- and CCR2-mediated processes is that both are triggered by autophagy deficiency, and thus can be considered as part of the overall tumorigenesis program under this condition, which may compensate for the lack of autophagy-directed metabolic advantage for aggressive growth.[41] The tumor surveillance function of autophagy thus can be at both the initiation and promotion stage (Figure 17*C*). These observations may facilitate the development of novel therapeutic approaches to inhibit these extrinsic mechanisms for cancer treatment.

Materials and Methods
Mice Used in the Study

The liver-specific autophagy-deficient mice, *Atg7^Δhep^* and *Atg5^Δhep^*, were generated by crossing *Atg7^fl/fl^*[15] and *Atg5^fl/fl^*[19] with Albumin-Cre recombinase transgenic mice (The Jackson Laboratory, Bar Harbor, ME). The inducible strains were generated by crossing the floxed mice with Albumin-Cre recombinase-estrogen receptor^T2^ transgenic mice.[17] To induce gene deletion, tamoxifen (Sigma-Aldrich, St. Louis, MO) was administered (6.0 mg/day, subcutaneously for 2 days). Mice deficient in *Ccr2* (cat no. 027619; The Jackson Laboratory), *Nrf2*, *Hmgb1*, or *Rage* have been reported.[17,42] These
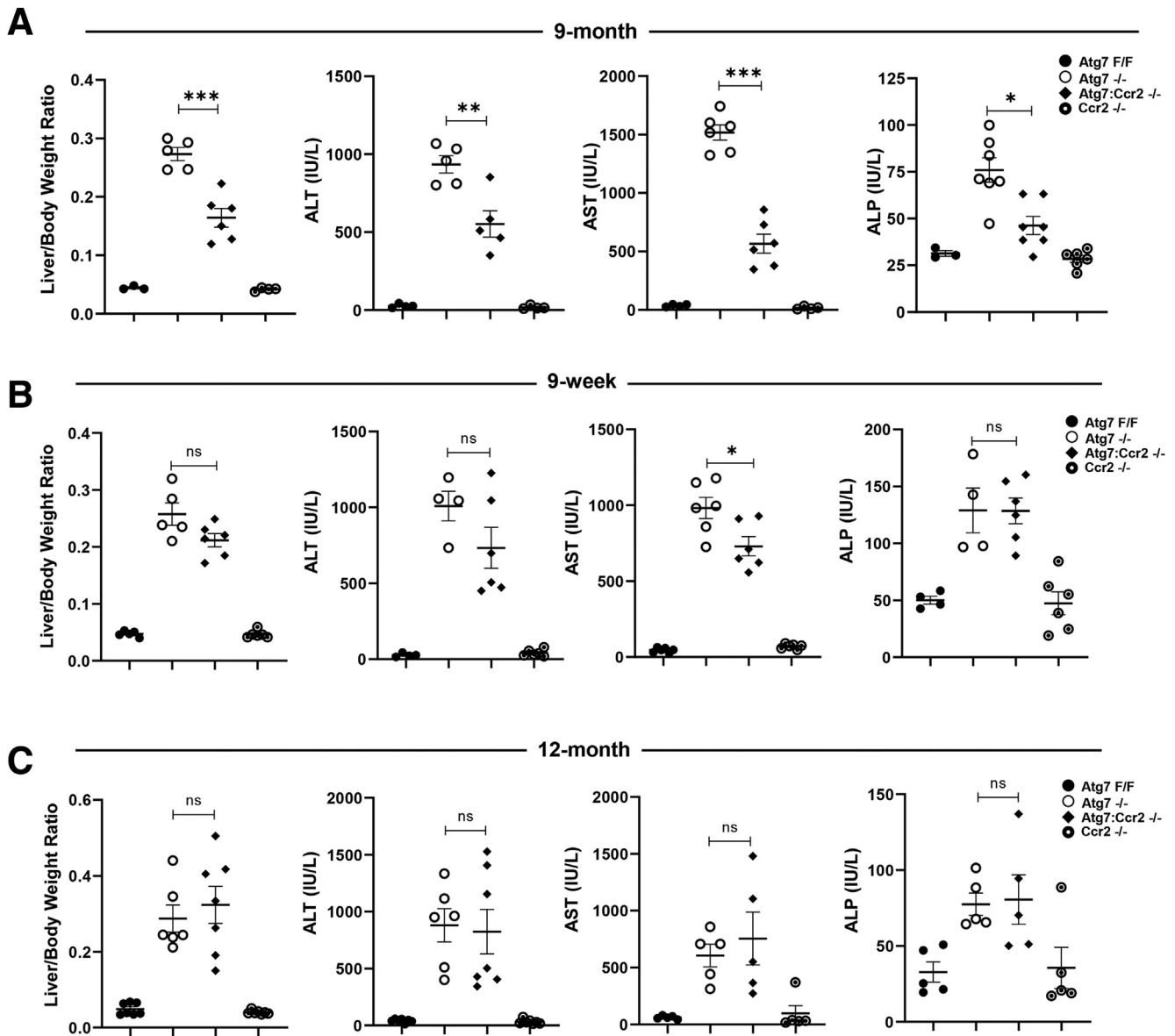
Figure 15. Deletion of _Ccr2_ differentially affects liver injury. The liver/body weight ratio and the serum levels of liver enzymes in (_A_) 9-month-old, (_B_) 9-week-old, or (_C_) 12-month-old mice of the designated genotypes. *_P_ < .05, **_P_ < .01, and ***_P_ < .001.

mice were crossed with _Atg7^Δhep^_ mice to generate doubly mutated strains. Mice were maintained on a 12-hour dark/light cycle with free access to chow diet and water. Both male and female mice (age, 3–16 wk) were used in the study. All animal procedures were approved by the Animal Care and Use Committee at Indiana University and Tulane University.

Antibodies and Nucleic Acid Primers

The antibodies and nucleic acid primers are listed in Tables 1 and 2, respectively.

Biochemical Analysis

Serum levels of alanine aminotransferase, aspartate aminotransferase, and alkaline phosphatase were measured per the manufacturer's protocols (Pointe Scientific, Canton, MI). Measurement of 4-hydroxyproline in liver tissues was performed using a hydroxyproline colorimetric assay kit (Biovision, Milpitas, CA). Liver tissue triglyceride and cholesterol levels were determined as previously described.[18] Lipid peroxidation was determined based on the level of malondialdehyde as described previously.[43] The serum level of CCL2 was assessed using an enzyme-linked immunosorbent assay kit (cat no. LS-F271; LSBio, Seattle, WA).

β-Galactosidase Activity Assay

The assay was conducted using the Cellular Senescence Assay Kit (cat no. KAA002; Millipore-Sigma, Burlington, MA). Briefly, frozen sections were washed with
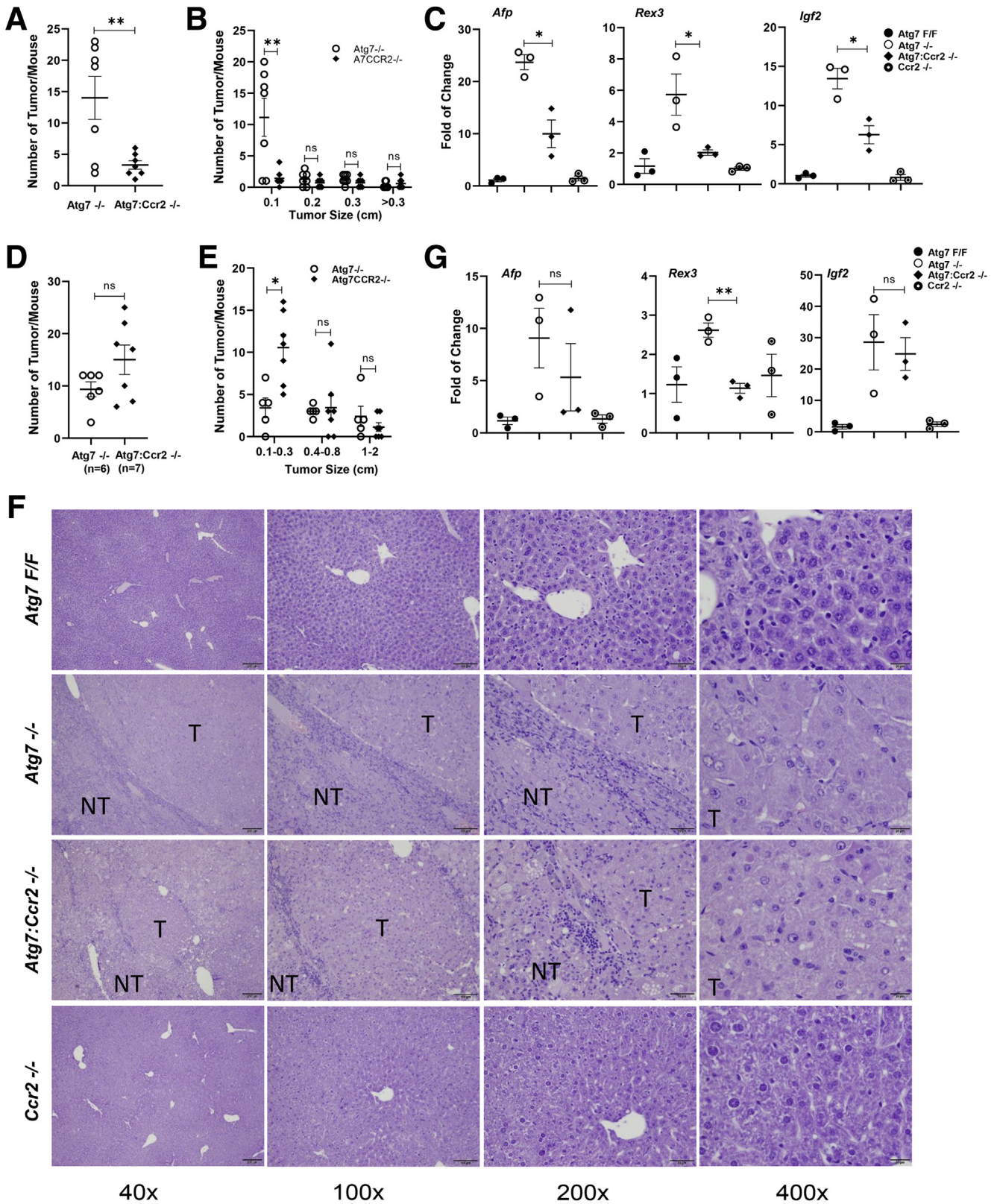
Figure 16. Deletion of *Ccr2* differentially affects liver tumor development. (*A*) Average numbers of hepatic tumors per mouse and (*B*) tumor size distribution, and (*C*) hepatic mRNA expression of oncofetal genes in 9-month-old mice. (*D*) Average numbers of hepatic tumors per mouse and (*E*) tumor size distribution in 12-month-old mice. (*F*) Representative H&E-stained micrographs of livers with different genotypes. The images were obtained at magnifications of 40× to 400×. (*G*) Hepatic mRNA expression of the oncofetal genes from 12-month-old mice of the designated genotypes (n = 3). *$P < .05$, **$P < .01$. T, tumor area; NT, nontumor area.

Table 1. Antibodies Used in Immunologic Assays

Antibody/host	Source/catalogue number/dilution
8-OHdG/mouse	Santa Cruz (Dallas, TX)/Sc-66036(15A3)/1:250
Alexa-488-goat anti-rabbit	Invitrogen (Carlsbad, CA)/A-11034/1:500
CCL2 (mouse specific)/rabbit	Cell Signaling (Danvers, MA)/2029/1:1000
CD3/rat	BD Pharmagen (San Diego, CA)/557306/1:100
CD11b	Novus (Centennial, CO)/NB110-89474/1:200
CD45R/rat	BD Pharmagen (San Diego, CA)/553089/1:100
Cy3-goat anti-rat	Jackson ImmunoResearch Laboratories, Inc (West Grove, PA)/712-165-150/1:500
FOXK1/rabbit	Cell Signaling (Danvers, MA)/12025/1:1000
GAPDH/mouse	Novus (Centennial, CO)/NB300-21/1:3000
GATA4/mouse	Santa Cruz (Dallas, TX)/Sc25310(G-4)/1:500
HRP-labeled goat anti-mouse secondary antibody	Jackson ImmunoResearch Laboratories, Inc (West Grove, PA)/705-165-147/1:5000
HRP-labeled goat anti-rabbit secondary antibody	Jackson ImmunoResearch Laboratories, Inc (West Grove, PA)/111-035-045/1:5000
Histone H3	Cell Signaling (Danvers, MA)/4499/1:2000
p15/rabbit	Novus (Centennial, CO)/NB100-91906/1:500
p21/rabbit	Santa Cruz (Dallas, TX)/Sc397(c-19)/1:200
p21/rat	Abcam (Waltham, Boston)/HUGO291/1:50
p62/SQSTM1/mouse	Abnova (Fisher Scientific, Pittsburgh, PA)/H00008878-M01/1:1000
p65/RELA (D14E12)/rabbit	Cell Signaling (Danvers, MA)/8242/1:1000
p-ATM (S1981)/mouse	EMB Millipore (Billerica, MA)/MAB3806/1:500
p-FOXK1 (S428)/rabbit	Nakatsumi et al,[28]/1:1000
Phospho-histone H2A.X (Ser139)/rabbit	Cell Signaling (Danvers, MA)/9718/1:400
PP2A (A subunit)/rabbit	Cell Signaling (Danvers, MA)/2039/1:1000
PP2A (B subunit)/rabbit	Cell Signaling (Danvers, MA)/4953/1:1000
PP2A (C subunit)/rabbit	Cell Signaling (Danvers, MA)/2038/1:1000
Sox9/rabbit	EMB Millipore (Billerica, MA)/AB5535/1:1000
TP53 (D2H90)/rabbit	Cell Signaling (Danvers, MA)/32532/1:1000
TP53-acetylated/rabbit	Millipore Sigma (Burlington, MA)/06-758/1:1000
β-actin/mouse	Sigma (Burlington, MA)/5441/1:5000
Vinculin	Novus (Centennial, CO)/NBP2-20859/1:2000

GAPDH, glyceraldehyde-3-phosphate dehydrogenase; HRP, horseradish peroxidase; 8-OHdG, 8-Hydroxy-2-deoxyguanosine.

phosphate-buffered saline (PBS), fixed in formalin, washed, and incubated overnight at 37°C with a staining solution containing 5-bromo-4-chloro-3-indolyl-βD-galactopyranoside, which, upon the effect of a lysosomal hydrolase active in senescent cells at pH 6.0, produces a blue precipitate, which was detected by light microscopy.[44]

Liver Perfusion and Cellular Separation of Parenchymal and Nonparenchymal Cells

Livers were subjected to the standard reverse perfusion as described previously.[43] Liver cells recovered from perfused livers were centrifuged to separate the parenchymal cells (containing hepatocytes) from the nonparenchymal cells.

Histology and Immunostaining Analysis

Liver tissues were fixed in 10% formalin and the paraffin-embedded sections were subjected to H&E, and other special staining. For immunofluorescence study, paraffin-embedded sections were deparaffinized and treated with antigen retrieval using citrate buffer (pH 6.0). Either deparaffinized–antigen-retrieved slides or frozen sections were permeabilized and blocked with 5% goat or donkey serum in PBS containing 0.1% Triton X-100 (MilliporeSigma, Burlington, MA) and 0.1 mol/L glycine for 1 hour, followed by incubation overnight at 4°C with primary antibodies diluted in PBS. Sections were washed in PBS containing 0.1% Triton X-100, followed by incubation with fluorochrome-conjugated secondary antibodies, and counterstained with Hoechst 33342 (1 μg/mL) for the nucleus. All images were obtained using a Nikon (Melville, NY) or Olympus (Center Valley, PA) microscope with epi-immunofluorescence capability and analyzed with the companion software.

Immunoblotting Analysis

Immunoblotting analysis was performed following the protocol published previously.[16] The images were digitally
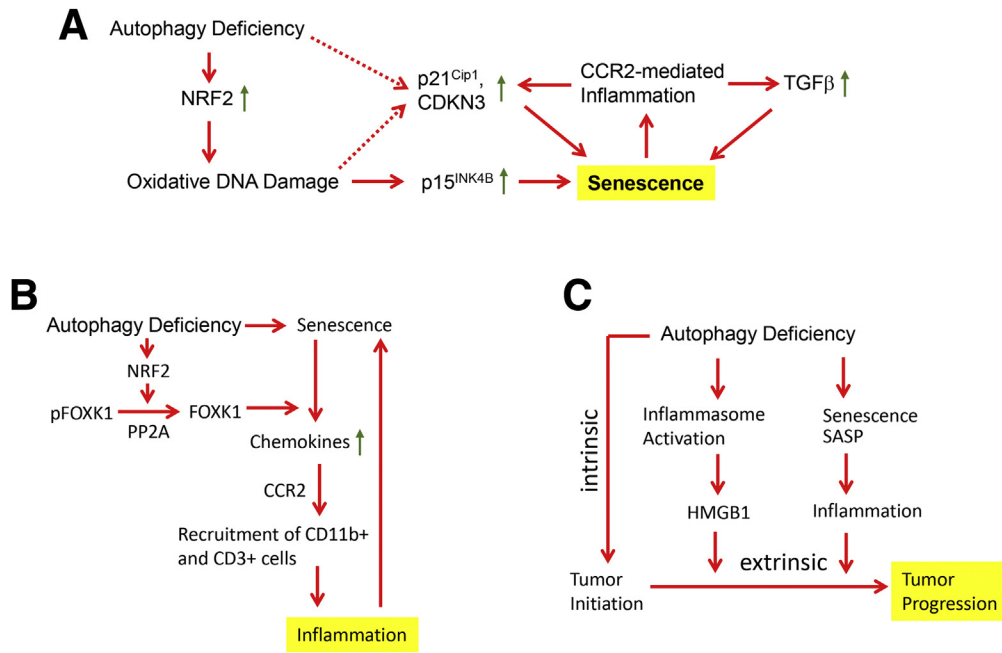
Figure 17. Working models on the crosstalk between autophagy deficiency, senescence, SASP, inflammation, and tumor development. (*A*) Hepatic autophagy deficiency causes NRF-2–dependent oxidative DNA damage, which leads to up-regulation of the CDKi p15/CDKN2b, senescence, and SASP. SASP/CCR2-mediated inflammation contributes to the up-regulation of p21/CDKN1a, CDKN3, and transforming growth factor (TGF)β, which further enhance senescence in an amplification loop. Up-regulation of p21/CDKN1b and CDKN3 could be regulated by factors in addition to NRF2 (*dashed arrows*). TGF-β could enhance senescence via p21/CDKN1a and/or p15/CDKN2b. These senescence mechanisms are intertwined under the influence of autophagy deficiency. (*B*) SASP in the context of hepatic autophagy deficiency is correlated with the NRF2-dependent activation of FOXK1, but not NF-κB and other pathways. The SASP is dominated by chemokines, which results in recruitment of inflammatory cells and parenchymal inflammation. Notably, CCR2-mediated inflammation could further enhance senescence and SASP, which amplifies inflammation in the liver. (*C*) Autophagy is a tumor-suppressive mechanism and autophagy deficiency can lead to tumor initiation intrinsically. Additional adverse effects caused by autophagy deficiency can further promote tumor progression extrinsically. These effects include the release of HMGB1 through the activation of inflammasome and the activation of SASP-induced inflammation. Thus, autophagy regulates tumorigenesis from initiation to progression.

acquired with a Kodak Image Station 4000 or a Bio-Rad ChemiDoc Image System. Densitometric analysis was performed using the companion software, and the values were normalized to the loading control (β-actin, glyceraldehyde-3-phosphate dehydrogenase, β-tubulin, heat shock protein 90, or histone H3) and then converted to units relative to the control.

Real-Time PCR

Total RNA was extracted from the liver tissue using the GeneJET RNA Purification Kit (cat no. K0732; Thermo Fisher Scientific, Carlsbad, CA). The complementary DNA was synthesized from 1.0 μg total RNA using a M-MLV Reverse Transcriptase Enzyme System (cat no. 28025-013; Life Technologies, Thermo Fisher Scientific, Carlsbad, CA). The real-time quantitative PCR was performed using SYBR Green Master Mixes on a 7500 FAST Real-Time PCR System (cat no. A46109; Life Technologies–Applied Biosystems, Thermo Fisher Scientific, Carlsbad, CA). Gene expression was calculated using the $2^{-\text{delta-delta } Ct}$ method and normalized to the housekeeping gene β-actin.

Statistical Analysis

Statistical analysis was performed using SigmaStat 3.5 (Systat Software Inc. San Jose, CA). All data are presented as means $\pm$ SEM. The numbers of mice used in individual experiments are shown in the figure legends. *P* values from at least 3 independent determinations or samples were calculated using a 2-tailed Student *t* test (for paired group comparisons) or 1-way analysis of variance with the appropriate post hoc analysis (for multigroup comparisons). A *P* value of less than .05 was considered statistically significant.

Table 2. Primers Used in PCR Assays

Gene name	Forward primer (5'→3')	Reverse primer (5'→3')
Afp	CTCAGCGAGGAGAAATGGTC	GAGTTCACAGGGCTTGCTTC
Albumin	GACGTGTGTTGCCGATGAGT	GTTTTCACGGAGGTTTGGAATG
Ccl1	GGCTGCCGTGTGGATACAG	AGGTGATTTTGAACCCACGTTT
Ccl2	TTAAAAACCTGGATCGGAACCAA	GCATTAGCTTCAGATTTACGGGT
Ccl3	TTCTCTGTACCATGACACTCTGC	CGTGGAATCTTCCGGCTGTAG
Ccl7	GCTGCTTTCAGCATCCAAGTG	CCAGGGACACCGACTACTG
Ccl8	TCTACGCAGTGCTTCTTTGCC	AAGGGGGATCTTCAGCTTTAGTA
Ccl11	GAATCACCAACAACAGATGCAC	ATCCTGGACCCACTTCTTCTT
Ccl12	ATTTCCACACTTCTATGCCTCCT	ATCCAGTATGGTCCTGAAGATCA
Cdkn3	ACCCTGATACATTGTTACGGAGG	CTCGAAGGCTGTCTATGGCTT
Col1a1	ACGGCTGCACGAGTCACAC	GGCAGGCGGGAGGTCTT
Cxcl14	GAAGATGGTTATCGTCACCACC	CGTTCCAGGCATTGTACCACT
Foxk1	ACCCACGAATAGCTTGACTGG	GCATTAGCGGCTACTGAGACG
Gata4	CCCTACCCAGCCTACATGG	ACATATCGAGATTGGGGTGTCT
Hp1γ	ATGGCCTCCAATAAAACTACATTG	CTCCACCTTCCCATTCACTAC
Igf2	TGAGAAGCACCAACATCGAC	CTTCTCCTCCGATCCTCCTG
Il4	GGTCTCAACCCCCAGCTAGT	GCCGATGATCTCTCTCAAGTGAT
Il6	TAGTCCTTCCTACCCCAATTTCC	TTGGTCCTTAGCCACTCCTTC
Mdm2	AGTCTCTGGACTCGGAAGATTA	CTGTATCGCTTTCTCCTGTCTG
Mmp12	CTGCTCCCATGAATGACAGTG	AGTTGCTTCTAGCCCAAAGAAC
Mmp13	CTTCTTCTTGTTGAGCTGGACTC	CTGTGGAGGTCACTGTAGACT
NFκB1/p50	ATGGCAGACGATGATCCCTAC	TGTTGACAGTGGTATTTCTGGTG
NFκB2/p52	GGCCGGAAGACCTATCCTACT	CTACAGACACAGCGCACACT
p15	GGCAAGTGGAGACGGTG	GTTGGGTTCTGCTCCGTG
p16-Set 1	TTTCGGTCGTACCCCGATTC	TGCACCGTAGTTGAGCAGAAGAG
p16-Set 2	CGTACCCCGATTCAGGTGAT	TTGAGCAGAAGAGCTGCTACGT
p16-Set 3	CGCAGGTTCTTGGTCACTGT	TGTTCACGAAAGCCAGAGCG
p16-Set 4	AACTCTTTCGGTCGTACCCC	GCGTGCTTGAGCTGAAGCTA
p18	GCAACTAATCGTCTTTTCCCG	AATCCATTTTGAGCGTTGACG
p19	CTTCATCGGGAGCTGGTG	AGGCATCTTGGACATTGGG
p21	CTTGCACTCTGGTGTCTGAG	GCACTTCAGGGTTTTCTCTTG
p27	TGGACCAAATGCCTGACTC	GGGAACCGTCTGAAACATTTTC
p57	CAGGACGAGAATCAAGAGCAG	CGACGCCTTGTTCTCCTG
RelA/p65	AGGCTTCTGGGCCTTATGTG	TGCTTCTCTCGCCAGGAATAC
Rex3	TACTCCTGGGCCTATCCTTG	GCAGCAGGAGGAGGAAGAG
Tgf-β	CCTGAGTGGCTGTCTTTTGA	CGTGGAGTTTGTTATCTTTGCTG
Tp53	ATGTTCCGGGAGCTGAATG	CCCCACTTTCTTGACCATTG
Traf3ip2	TCCCGTGGAGGTTGATGAATC	TCAGGGTGCCTTCTAAAGAAACT
α-Sma	ATCGTCCACCGCAAATGC	AAGGAACTGGAGGCGCTG
β-actin	GACGGCCAGGTCATCACTATTG	AGGAAGGCTGGAAAAGAGCC

References

1. He S, Sharpless NE. Senescence in health and disease. Cell 2017;169:1000–1011.
2. Huda N, Liu G, Hong H, Yan S, Khambu B, Yin XM. Hepatic senescence, the good and the bad. World J Gastroenterol 2019;25:5069–5081.
3. Frey N, Venturelli S, Zender L, Bitzer M. Cellular senescence in gastrointestinal diseases: from pathogenesis to therapeutics. Nat Rev Gastroenterol Hepatol 2018; 15:81–95.
4. Paradis V, Youssef N, Dargere D, Ba N, Bonvoust F, Deschatrette J, Bedossa P. Replicative senescence in normal liver, chronic hepatitis C, and hepatocellular carcinomas. Hum Pathol 2001; 32:327–332.
5. Wiemann SU, Satyanarayana A, Tsahuridu M, Tillmann HL, Zender L, Klempnauer J, Flemming P, Franco S, Blasco MA, Manns MP, Rudolph KL. Hepatocyte telomere shortening and senescence are general markers of human liver cirrhosis. FASEB J 2002; 16:935–942.

6. Gutierrez-Reyes G, del Carmen Garcia de Leon M, Varela-Fascinetto G, Valencia P, Perez Tamayo R, Rosado CG, Labonne BF, Rochilin NM, Garcia RM, Valadez JA, Latour GT, Corona DL, Diaz GR, Zlotnik A, Kershenobich D. Cellular senescence in livers from children with end stage liver disease. PLoS One 2010;5:e10231.

7. Ferreira-Gonzalez S, Lu WY, Raven A, Dwyer B, Man TY, O'Duibhir E, Lewis PJS, Campana L, Kendall TJ, Bird TG, Tarrats N, Acosta JC, Boulter L, Forbes SJ. Paracrine cellular senescence exacerbates biliary injury and impairs regeneration. Nat Commun 2018;9:1020.

8. Krizhanovsky V, Yon M, Dickins RA, Hearn S, Simon J, Miething C, Yee H, Zender L, Lowe SW. Senescence of activated stellate cells limits liver fibrosis. Cell 2008; 134:657–667.

9. Klionsky DJ, Petroni G, Amaravadi RK, Baehrecke EH, Ballabio A, Boya P, Bravo-San Pedro JM, Cadwell K, Cecconi F, Choi AMK, Choi ME, Chu CT, Codogno P, Colombo MI, Cuervo AM, Deretic V, Dikic I, Elazar Z, Eskelinen EL, Fimia GM, Gewirtz DA, Green DR, Hansen M, Jaattela M, Johansen T, Juhasz G, Karantza V, Kraft C, Kroemer G, Ktistakis NT, Kumar S, Lopez-Otin C, Macleod KF, Madeo F, Martinez J, Melendez A, Mizushima N, Munz C, Penninger JM, Perera RM, Piacentini M, Reggiori F, Rubinsztein DC, Ryan KM, Sadoshima J, Santambrogio L, Scorrano L, Simon HU, Simon AK, Simonsen A, Stolz A, Tavernarakis N, Tooze SA, Yoshimori T, Yuan J, Yue Z, Zhong Q, Galluzzi L, Pietrocola F. Autophagy in major human diseases. EMBO J 2021;40:e108863.

10. Boya P, Reggiori F, Codogno P. Emerging regulation and functions of autophagy. Nat Cell Biol 2013;15:713–720.

11. Czaja MJ, Ding WX, Donohue TM Jr, Friedman SL, Kim JS, Komatsu M, Lemasters JJ, Lemoine A, Lin JD, Ou JH, Perlmutter DH, Randall G, Ray RB, Tsung A, Yin XM. Functions of autophagy in normal and diseased liver. Autophagy 2013;9:1131–1158.

12. Madrigal-Matute J, Cuervo AM. Regulation of liver metabolism by autophagy. Gastroenterology 2016; 150:328–339.

13. Khambu B, Yan S, Huda N, Liu G, Yin XM. Homeostatic role of autophagy in hepatocytes. Semin Liver Dis 2018; 38:308–319.

14. Komatsu M, Waguri S, Ueno T, Iwata J, Murata S, Tanida I, Ezaki J, Mizushima N, Ohsumi Y, Uchiyama Y, Kominami E, Tanaka K, Chiba T. Impairment of starvation-induced and constitutive autophagy in Atg7-deficient mice. J Cell Biol 2005;169:425–434.

15. Komatsu M, Kurokawa H, Waguri S, Taguchi K, Kobayashi A, Ichimura Y, Sou YS, Ueno I, Sakamoto A, Tong KI, Kim M, Nishito Y, Iemura S, Natsume T, Ueno T, Kominami E, Motohashi H, Tanaka K, Yamamoto M. The selective autophagy substrate p62 activates the stress responsive transcription factor Nrf2 through inactivation of Keap1. Nat Cell Biol 2010;12:213–223.

16. Ni HM, Woolbright BL, Williams J, Copple B, Cui W, Luyendyk JP, Jaeschke H, Ding WX. Nrf2 promotes the development of fibrosis and tumorigenesis in mice with defective hepatic autophagy. J Hepatol 2014; 61:617–625.

17. Khambu B, Huda N, Chen XY, Antoine DJ, Li Y, Dai GL, Kohler UA, Zong WX, Waguri S, Werner S, Oury TD, Gong Z, Yin XM. HMGB1 promotes ductular reaction and tumorigenesis in autophagy-deficient livers. J Clin Invest 2018;128:2419–2435.

18. Khambu B, Li T, Yan S, Yu C, Chen X, Goheen M, Li Y, Lin J, Cummings OW, Lee YA, Friedman S, Dong Z, Feng GS, Wu S, Yin XM. Hepatic autophagy deficiency compromises farnesoid X receptor functionality and causes cholestatic injury. Hepatology 2019; 69:2196–2213.

19. Takamura A, Komatsu M, Hara T, Sakamoto A, Kishi C, Waguri S, Eishi Y, Hino O, Tanaka K, Mizushima N. Autophagy-deficient mice develop multiple liver tumors. Genes Dev 2011;25:795–800.

20. Sulli G, Di Micco R, di Fagagna FD. Crosstalk between chromatin state and DNA damage response in cellular senescence and cancer. Nat Rev Cancer 2012; 12:709–720.

21. Narita M, Nunez S, Heard E, Narita M, Lin AW, Hearn SA, Spector DL, Hannon GJ, Lowe SW. Rb-mediated heterochromatin formation and silencing of E2F target genes during cellular senescence. Cell 2003; 113:703–716.

22. Zhang R, Poustovoitov MV, Ye X, Santos HA, Chen W, Daganzo SM, Erzberger JP, Serebriiskii IG, Canutescu AA, Dunbrack RL, Pehrson JR, Berger JM, Kaufman PD, Adams PD. Formation of MacroH2A-containing senescence-associated heterochromatin foci and senescence driven by ASF1a and HIRA. Dev Cell 2005;8:19–30.

23. Marechal A, Zou L. DNA damage sensing by the ATM and ATR kinases. Cold Spring Harb Perspect Biol 2013; 5:a012716.

24. Struthers L, Patel R, Clark J, Thomas S. Direct detection of 8-oxodeoxyguanosine and 8-oxoguanine by avidin and its analogues. Anal Biochem 1998;255:20–31.

25. Lopes-Paciencia S, Saint-Germain E, Rowell MC, Ruiz AF, Kalegari P, Ferbeyre G. The senescence-associated secretory phenotype and its regulation. Cytokine 2019;117:15–22.

26. Hayden MS, Ghosh S. NF-kappa B, the first quarter-century: remarkable progress and outstanding questions. Gene Dev 2012;26:203–234.

27. Kang C, Xu Q, Martin TD, Li MZ, Demaria M, Aron L, Lu T, Yankner BA, Campisi J, Elledge SJ. The DNA damage response induces inflammation and senescence by inhibiting autophagy of GATA4. Science 2015; 349:aaa5612.

28. Nakatsumi H, Matsumoto M, Nakayama KI. Noncanonical pathway for regulation of CCL2 expression by an mTORC1-FOXK1 axis promotes recruitment of tumor-associated macrophages. Cell Rep 2017;21:2471–2486.

29. Hughes CE, Nibbs RJB. A guide to chemokines and their receptors. FEBS J 2018;285:2944–2971.

30. Ingersoll MA, Platt AM, Potteaux S, Randolph GJ. Monocyte trafficking in acute and chronic inflammation. Trends Immunol 2011;32:470–477.

31. Loyher PL, Rochefort J, Baudesson de Chanville C, Hamon P, Lescaille G, Bertolus C, Guillot-Delost M,

Krummel MF, Lemoine FM, Combadiere C, Boissonnas A. CCR2 influences T regulatory cell migration to tumors and serves as a biomarker of cyclophosphamide sensitivity. Cancer Res 2016;76:6483–6494.

32. Hannon GJ, Beach D. P15(Ink4b) is a potential effector of Tgf-beta-induced cell-cycle arrest. Nature 1994;371:257–261.

33. Khambu B, Hong H, Liu S, Liu G, Chen X, Dong Z, Wan J, Yin XM. The HMGB1-RAGE axis modulates the growth of autophagy-deficient hepatic tumors. Cell Death Dis 2020;11:333.

34. Young AR, Narita M, Ferreira M, Kirschner K, Sadaie M, Darot JF, Tavare S, Arakawa S, Shimizu S, Watt FM, Narita M. Autophagy mediates the mitotic senescence transition. Genes Dev 2009;23:798–803.

35. Kang HT, Lee KB, Kim SY, Choi HR, Park SC. Autophagy impairment induces premature senescence in primary human fibroblasts. PLoS One 2011;6:e23367.

36. Garcia-Prat L, Martinez-Vicente M, Perdiguero E, Ortet L, Rodriguez-Ubreva J, Rebollo E, Ruiz-Bonilla V, Gutarra S, Ballestar E, Serrano AL, Sandri M, Munoz-Canoves P. Autophagy maintains stemness by preventing senescence. Nature 2016;529:37–42.

37. Rayess H, Wang MB, Srivatsan ES. Cellular senescence and tumor suppressor gene p16. Int J Cancer 2012;130:1715–1725.

38. Bantubungi K, Hannou SA, Caron-Houde S, Vallez E, Baron M, Lucas A, Bouchaert E, Paumelle R, Tailleux A, Staels B. Cdkn2a/p16Ink4a regulates fasting-induced hepatic gluconeogenesis through the PKA-CREB-PGC1alpha pathway. Diabetes 2014;63:3199–3209.

39. Yuan H, Xu Y, Luo Y, Wang NX, Xiao JH. Role of Nrf2 in cell senescence regulation. Mol Cell Biochem 2021;476:247–259.

40. White E, DiPaola RS. The double-edged sword of autophagy modulation in cancer. Clin Cancer Res 2009;15:5308–5316.

41. Goldsmith J, Levine B, Debnath J. Autophagy and cancer metabolism. Methods Enzymol 2014;542:25–57.

42. Satpathy AT, Briseno CG, Lee JS, Ng D, Manieri NA, Kc W, Wu X, Thomas SR, Lee WL, Turkoz M, McDonald KG, Meredith MM, Song C, Guidos CJ, Newberry RD, Ouyang W, Murphy TL, Stappenbeck TS, Gommerman JL, Nussenzweig MC, Colonna M, Kopan R, Murphy KM. Notch2-dependent classical dendritic cells orchestrate intestinal immunity to attaching-and-effacing bacterial pathogens. Nat Immunol 2013;14:937–948.

43. Ding WX, Li M, Chen X, Ni HM, Lin CW, Gao W, Lu B, Stolz DB, Clemens DL, Yin XM. Autophagy reduces acute ethanol-induced hepatotoxicity and steatosis in mice. Gastroenterology 2010;139:1740–1752.

44. Dimri GP, Lee XH, Basile G, Acosta M, Scott C, Roskelley C, Medrano EE, Linskens M, Rubelj I, Pereirasmith O, Peacocke M, Campisi J. A biomarker that identifies senescent human-cells in culture and in aging skin in-vivo. Proc Natl Acad Sci U S A 1995;92:9363–9367.

Correspondence
Address correspondence to: Xiao-Ming Yin, MD, PhD, Department of Pathology and Laboratory Medicine, Tulane University School of Medicine, New Orleans, Louisiana 70112. e-mail: xmyin@tulane.edu; fax: (504) 988-7389.